NASA CR-151461
ERIM 115800-49-F

NASA

Final Report

ACTIVE AND PASSIVE MULTISPECTRAL SCANNER FOR EARTH RESOURCES APPLICATIONS:

An Advanced Applications Flight Experiment

P.G. HASELL, Jr., L.M. PETERSON, F.J. THOMSON,
E.A. WORK, and F.J. KRIEGLER
Infrared & Optics Division
JUNE 1977

Prepared for
NATIONAL AERONAUTICS AND SPACE ADMINISTRATION

Lyndon B. Johnson Space Center
Houston, Texas 77058
Contract No. NAS9-14594
Technical Monitor: Jared R. Woodfill/ED6

ENVIRONMENTAL
RESEARCH INSTITUTE OF MICHIGAN
FORMERLY WILLOW RUN LABORATORIES, THE UNIVERSITY OF MICHIGAN
BOX 618 • ANN ARBOR • MICHIGAN 48107

TECHNICAL REPORT STANDARD TITLE PAGE

1. Report No.	2. Government Accession No.	3. Recipient's Catalog No.
NASA CR-ERIM 115800-49-F		

4. Title and Subtitle	5. Report Date
ACTIVE AND PASSIVE MULTISPECTRAL SCANNER FOR EARTH RESOURCES APPLICATIONS (An Advanced Applications Flight Experiment)	April 1977
	6. Performing Organization Code: 115800-49-F
7. Author(s) P. G. Hasell, Jr., L. M. Peterson, F. J. Thomson, E. A. Work and F. J. Kriegler	8. Performing Organization Report No.
9. Performing Organization Name and Address: Environmental Research Institute of Michigan, P. O. Box 618, Ann Arbor, Michigan 48107	10. Work Unit No.
	11. Contract or Grant No.: NAS9-14594
12. Sponsoring Agency Name and Address: National Aeronautics and Space Administration, Lyndon B. Johnson Space Center, Houston, Texas 77058	13. Type of Report and Period Covered: Final Report, June 12, 1975 through April 30, 1977
	14. Sponsoring Agency Code

15. Supplementary Notes

The work was performed for the Sensor Systems Development Branch. Mr. Jared R. Woodfill/ED6 was the technical monitor.

16. Abstract

This is the final report on the development of an experimental airborne multispectral scanner to provide both active (laser illuminated) and passive (solar illuminated) data from a commonly registered surface scene. The system was constructed according to specifications derived in an initial program design study. The system was installed in ERIM's aircraft and test flown to produce illustrative active and passive multispectral imagery. However, data was not collected nor analyzed for any specific application. It is anticipated that other contracts will support the use of the system which will remain at ERIM for exploration of the usefulness of combined active and passive data in various applications some of which are identified in the report.

17. Key Words	18. Distribution Statement
Airborne Sensor System Multispectral Scanner Active Scanning Active Imager Profiler	Initial distribution is indicated at the end of this document

19. Security Classif. (of this report)	20. Security Classif. (of this page)	21. No. of Pages	22. Price
Unclassified	Unclassified	ix + 93	

PREFACE

This final report is submitted in fulfillment of NASA Contract NAS 9-14594. Mr. Jared R. Woodfill of the Lyndon B. Johnson Space Center in Houston, Texas was the contract technical monitor. Messrs. Philip G. Hasell, Jr. and Fred J. Thomson directed the program as co-principal investigators at the Environmental Research Institute of Michigan (ERIM). The program was accomplished by ERIM's Infrared and Optics Division headed by Mr. Richard R. Legault.

The principal investigators wish to acknowledge the help of the following persons who made significant contributions in the development of the system:

John E. Colwell	Applications analysis, vegetation
Neil V. Griffin	Laser cooling equipment fabrication
William J. Juodawlkis	Electronic equipment fabrication and operation
Ernest L. Kraudelt	Mechanical fabrication
Frank J. Kriegler	Signal handling design
Jimmie C. Ladd	System integration and operation
Leo M. Larsen	System design and performance
David R. Lyzenga	Applications analysis, water
Lauren M. Peterson	Laser systems design and operation
Edgar A. Work	Mechanical design

CONTENTS

FIGURES

TABLES

SUMMARY

The original objective of this program was to demonstrate that the proper combination of active and passive multispectral scanner data could be processed to enhance remote sensing capabilities for earth resources applications. The eventual program fell short of demonstrating capabilities in applications analysis, but it did produce an airborne 12-channel, active and passive multispectral scanner system which was successfully test flown to produce illustrative imagery. Samples of this imagery are shown in Figures 1 and 2.

Only one of the two active bands were operative in the test flights although both bands have operated satisfactorily in subsequent data collection operations in support of other programs. Selected laser illuminated scenes at 1.06 μm from the test flights are shown in Figure 1. Selected wavelength bands of passive imagery which is commonly registered with the active are shown in Figure 2. This imagery is typical of the 11 bands of passive imagery recorded simultaneously at visible and infrared wavelengths for this flight.

This experimental airborne instrumentation system will remain at ERIM after delivery to NASA. NASA's intent is to make this unique data collection capability available to users who may want to explore the value of active and passive data in their applications. ERIM's multispectral data processing and analysis capabilities can be used to evaluate the data in various applications. Not only can the system produce imagery, but in one mode of laser operation it can also produce surface reflectance as a function of surface penetration. This feature is useful in bathymetry and to determine vegetative canopy characteristics.

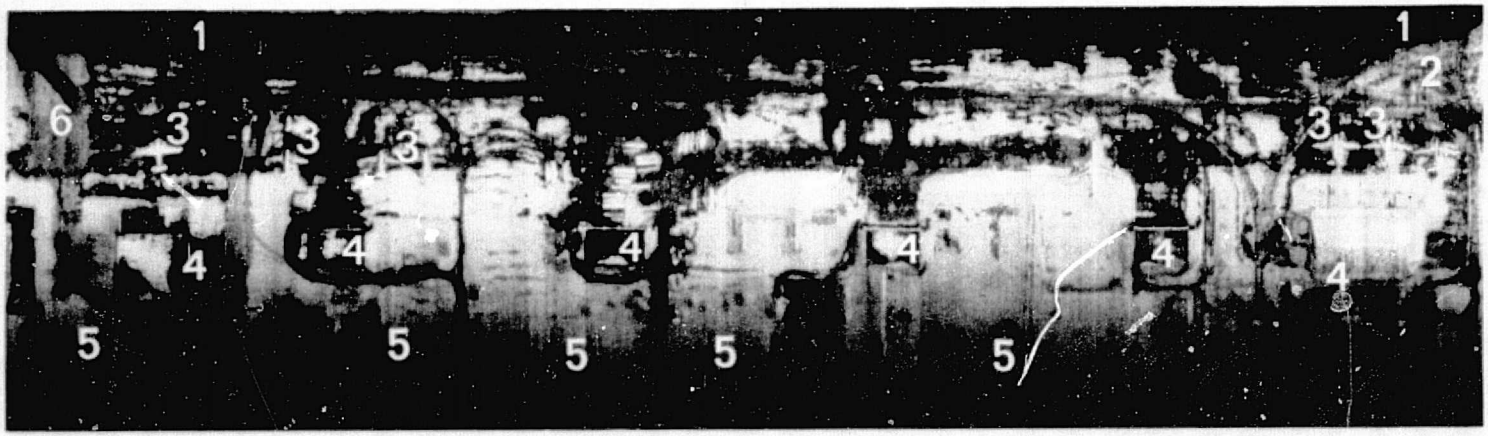

1. Blacktop Taxiway
2. Partially Snow Covered, Wet Concrete Ramp
3. Parked Aircraft
4. Hangar Buildings
5. Snow Covered Grass
6. Cleared, Dry Concrete Ramp

(a) Willow Run Ramp, 1000 ft., Late Afternoon on March 19

N →

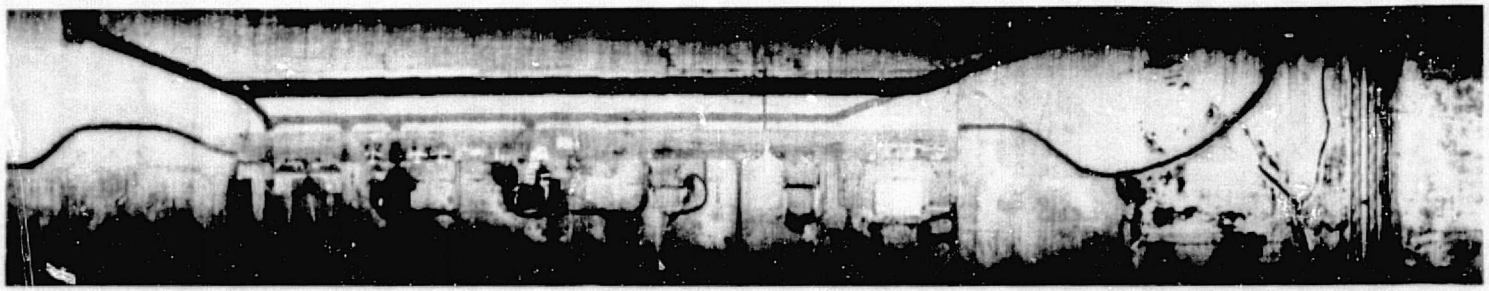

(b) Willow Run Ramp, 2000 ft., Late Night on March 25
Surface Clear and Dry (No Snow)

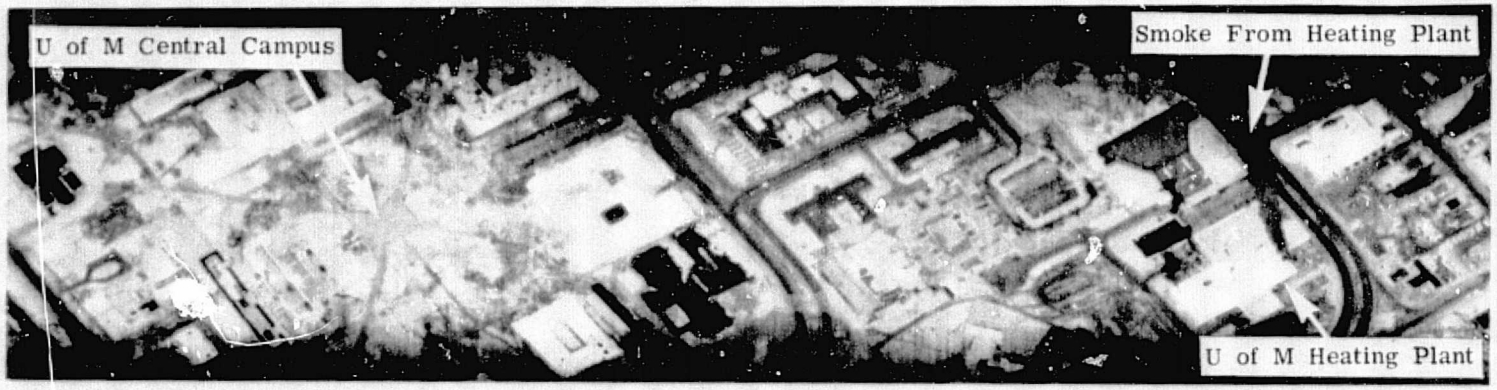

(c) Ann Arbor, 1000 ft., Late Night on March 25
Surface Clear and Dry (No Snow)

FIGURE 1. ACTIVE IMAGERY, 1.06 μm WAVELENGTH.

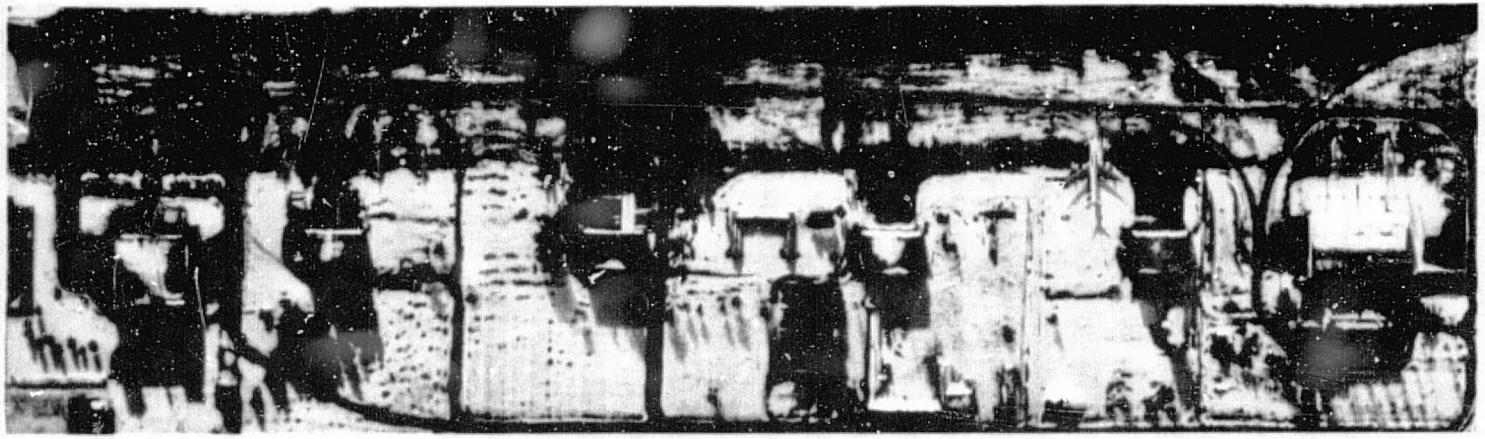

(a) 0.4 - 0.7 μm Active Receiver No. 2 with Filter Removed, Late Afternoon on March 19.
Surface Wet with Melting Snow Cover

N →

(b) Spectrometer: 0.48-0.53 μm (Typical of 9 Bands), Late Afternoon on March 19.
Surface Wet with Melting Snow Cover

(c) Infrared Detector: 9.0-11.4 μm (Thermal), Late Night on March 25
Surface Clear and Dry (No Snow)

FIGURE 2. PASSIVE IMAGERY OF WILLOW RUN RAMP FROM 1000 FT.

1.
INTRODUCTION

This instrumentation development is the natural extension of the passive multispectral scanner technology advanced by ERIM with NASA support during the late 1960's and early 1970's. It follows the development trend at ERIM of military support of new ideas through the feasibility demonstration phase followed by NASA support in adapting the new technology to remote sensing applications.

The feasibility of an airborne scanner simultaneously providing active and passive imagery was first demonstrated by ERIM in the early 1970's. Military support of the technology development followed soon thereafter; NASA's interest commenced in 1974 with contract support of the concept development for earth resources applications beginning at ERIM in June 1975. This initial 18-month developmental contract was extended to 22 months. The results of program completion in April 1977 are reported herein.

An experimental 12-channel, active and passive multispectral scanner was developed and successfully flown in ERIM's aircraft to produce illustrative imagery. The system was designed to provide flexibility in the selection of various wavelengths for the two active and ten passive scanner channels. The wavelength bands can be selected in the ultraviolet, visible and infrared portions of the electromagnetic spectrum.

The initial system configuration provided one active band tunable in the visible and one in the near infrared (1.06 μm). The ten passive bands are in the visible and infrared region between 0.4 and 14.0 μm. The active illuminator in the visible is pulsed, providing a mode of operation where the reflected radiation can be examined as a function of surface penetration. At the designed operating altitude of 1000 ft., the system provides a two or three dimensional spatial resolution of about 2 ft over a swath width of 2000 ft. The scanner

data is radiometrically calibrated through reference to integral sources which are periodically compared with laboratory standards.

The objective of the program was to demonstrate that an active capability can be added to a passive multispectral scanner and that the combination will enhance the utility for earth resources applications. The active capability was added to the passive scanner but the utility of the combined data was not demonstrated as part of this program. It is anticipated that this utility will be demonstrated by ERIM in the use of the system equipment in support of other programs in the near future.

2.
PROGRAM DISCUSSION

The program commenced with a design study to identify system performance requirements for selected earth resources applications. These performance requirements were translated into equipment design parameters with some compromises made between desired performance and performance obtainable with available equipment. The system was configured around off-the-shelf components. No new developments were initiated other than the integration of available components into an operating system. Once the system was built, it was operated in ground and flight tests to demonstrate its performance. This development is discussed in the following sections.

2.1 APPLICATIONS REQUIREMENTS

The advantages of and unique information obtainable from laser illuminated (active) and solar illuminated (passive) data were determined in an applica ions study conducted during the first three months of the program. The study objective was to more precisely identify those applications (broadly subdivided into vegetation and water applications) which would benefit from information derived from active-passive data and to identify the sensor spectral bands, radiometric precision, and spatial resolution needed to achieve useful information. Once these sensor specifications were determined, the capabilities of existing lasers and scanner components were reviewed to determine available performance. Then a compromise system, one which supported both vegetation and water applications, was derived.

Throughout the design, we focused on defining the performance of the active and passive bands crucial to the applications selected. This in no way means that these are the only bands needed for the applications -- other passive bands are required, for example, to map vegetation types. The performance in the passive bands obtained from ERIM's M-7 multispectral scanner was judged adequate for these supporting functions.

Since the passive section of the active-passive scanner was nearly a carbon copy of the M-7 design, little effort was spent assessing performance requirements for the passive bands.

First, promising vegetation and water applications were identified for which active and passive data together provided new or much better information than passive data alone. Since the list of potential applications in each area was large, a subset of these applications was selected for in-depth study, using four criteria:

1. that there were a number of potential users for the information,
2. that the application was important to some set of potential federal and state government or private users,
3. that the active-passive data, suitably processed, could provide unique or better quality information than could be provided with other forms of remote sensing,
4. that there was high probability of successfully obtaining the information required using an active-passive scanner constructed with current technology.

Applying these criteria to the list of potential vegetation and water applications resulted in selection of four vegetation and three water applications for in-depth study.

Then, using mathematical models, we calculated the required system radiometric precision, spectral bands of operation, and spatial resolution, using the information requirements for a particular application and some typical flight altitudes, fields of view, and other sensor parameters. Separate optimum active-passive systems for vegetation and water applications were designed. Then a compromise system, consistent with available laser performance and weight, power, and cost limitations, was designed.

2.1.1 Vegetation Applications

Three of the four applications which were selected for study can be explored with this system.

1. Determination of percent vegetation cover or leaf area index at high values of these parameters as an indication of potential crop yield (e.g., wheat)
2. Determination of structure of a vegetation canopy, as an aid to better vegetation type mapping and crop condition assessment
3. Assessing conditions in two or more layers of a vegetation canopy, as an aid to disease or moisture stress detection
4. Topographic mapping (feasible, but not part of this system).

For the first three applications, the utility of 1.06 μm and 0.64 μm bands is apparent from Table 1. Table 1 shows the effects on canopy reflectance as important parameters of the canopy are varied. Both active and passive 1.06 μm and 0.64 μm data are required to determine the exact status of the canopy. The 1.06 μm energy penetrates the canopy (because the leaves are transparent at this wavelength) and offers the potential to map percentage cover and some canopy structural variations within canopies. The 0.64 μm band is in a spectral region where chlorophyll absorbs strongly. Plant diseases which result in destruction of leaf or stem chlorophyll will be effectively assessed by processing data collected in this spectral region. Imaging capability in these bands is highly desirable.

Because we are assessing crop and natural vegetation areas with considerable spatial structure (e.g., row crops or forest plantations) it is desirable to have a spatial resolution coarser than the spatial structure in the scene. For typical row crops, row spacings are on the order of 2-3 ft., hence, the spatial resolution should be coarser than this. A nominal value of 10 feet was judged adequate. Because active sensor radiometric precision actually improves as resolution is made finer (the ratio of laser power to solar power increases, thus improving the signal to noise ratio), a sensor resolution of 2 feet (equivalent

TABLE 1. ADVANTAGES OF TWO BAND IMAGING FOR AGRICULTURAL APPLICATIONS

	$\theta_s = 70^o$		$\theta_s = 70^o$	
	Active 1.06μm	Passive 1.06μm	Active 0.64μm	Passive 0.64μm
% Cover Decrease	-	-	+	+
Structure Change Increase v/h	0	+	0	-
Disease Lower Layer	0	0	÷	0
Disease Upper Layer	0	0	+	+

- = Reflectance Decrease

+ = Reflectance Increase

θ_s = Solar Zenith Angle

v/h = Ratio of vertical/horizontal projected leaf area

to a 2 mrad instantaneous field of view at 1000 ft. altitude) was selected. The selection was made as an engineering compromise between fine resolution and precision of alignment of laser illuminating source and receiver. The 10 ft. resolution would then be obtained by smoothing the scanner data by averaging 25 pixels (5x5) of 2 ft. resolution data.

The required radiometric precision for each band depends on which of the applications are considered. The required noise equivalent reflectance (NEΔP) for the active and passive bands is summarized in Table 2. Not all applications require both active or passive bands. Where data from an active band are required, a number appears in Table 2; where data from an active band are not needed, Table 2 is blank. The pacing performance requirements for all four applications are enclosed in boxes.

Thus an optimum system for vegetation applications would consist of a red band (0.64 μm) and infrared (1.06 μm) imager with 10 ft. linear ground resolution and noise equivalent reflectances of 0.9% and 0.2% respectively at 1000 ft. altitude, through an atmosphere of 10 km horizontal visibility. The corresponding performance required of the 0.8-1.0 μm passive band is 0.85% noise equivalent reflectance.

2.1.2 Water Applications

From a list of candidate water applications, three were selected for study using the criteria outlined earlier. The three applications were:

1. improved water depth mapping using pulsed laser signals to calibrate passive water depth mapping algorithms
2. assessment of the vertical distribution of sediment and of water attenuation and scattering coefficients
3. measurement of lower concentrations of Rhodamine WT dye (a common dye used to trace the movement of water masses) than can be detected by visual or photographic techniques.

TABLE 2. SUMMARY OF SCANNER ACTIVE CHANNEL PERFORMANCE REQUIREMENTS — VEGETATION APPLICATIONS

Application	Required Information and Precision	Implied Active Channel NEΔρ		Implied Passive Channel NEΔρ		Ancillary Conditions
		1.06 μm	0.64 μm	0.8–1 μm	0.64 μm	
Percent Cover Mapping	Percent cover ±2.5%(D), ±5%(M) at percent cover = 63%	1.59%(D) 3.14%(M)		[0.85%(D)] 1.7%(M)		1000 ft, solar zenith angle 45°, 10 km atmospheric visibility, nadir look, 10 ft resolution.
Canopy Structure Determination	Vertical/horizontal projected leaf area ratio, ±0.25(d), ±0.5(M) at H = 0.5, v/h = 2.5	1.59%(D) 3.14%(M)		1.35%(D) 2.7%(M)		As above but sun zenith angle of 70° for passive data
Disease in Lower Layers	Detect difference between Corn Blight levels 0 and 3(M)		[0.9%]			As for percent cover mapping.
Terrain or Vegetation Height	Terrain height ±1 m(M), Height of vegetation ±1 m or ±10% of height, whichever less (M)	[0.2%]				As for percent cover mapping with scene reflectance = 0.3.

D: desired

M: mandatory

[ ]: Critical data for each application

By contrast with the vegetation applications, bands in the 0.50-0.55 μm region are required for an active-passive system responsive to water applications requirements. The 0.50-0.55 μm region is one of maximum transparency of a wide range of water types. Because either depth, sediment profile, or fluorescence information is required, a pulsed system for obtaining the third-dimensional information (to complement the two-dimensional information obtainable with passive techniques) is most useful. Because of the high electronic bandwidth necessary to temporally resolve pulsed laser returns on a nanosecond time scale and the corresponding high peak power requirements of the pulsed-laser system, it is impractical to simply pulse modulate the lasers used for imaging. Likewise, those lasers constructed for pulse operation are capable of only small amounts of output power in the continuous wave (CW) mode. The conclusion is that a separate pulsed laser system is required. Such a laser system should have output in the 0.50-0.55 μm region and have a pulse width less than 9 nanoseconds to permit mapping of 1 m thick concentrations of sediment and a pulse width less than 5.4 nanoseconds to resolve 0.6 m water depths. A peak power output of 15 kw is required to satisfy most of the applications. High-speed signal processing and digitizing circuitry will be required to analyze the return pulse and to record the digitized pulse samples on magnetic tape.

For water applications, a spatial resolution of about 10 feet was judged adequate. The same considerations that applied to the vegetation applications apply to water applications -- that active scanner performance improves as the instantaneous field of view (IFOV) decreases. Consequently, for the water applications, we will operate with a 2 mrad IFOV for the pulsed laser system. This will yield 2 ft linear resolution at a flight altitude of 1000 ft.

The information requirements and the corresponding laser pulse lengths, wavelengths of operation, and peak power levels are shown in Table 3. As can be seen from Table 3, the peak power requirements for some applications are extremely high. A compromise was reached for water applications based on the use of nitrogen-laser-pumped dye laser with 15 kw of peak output power. This laser was the most powerful pulsed dye laser available from American sources at the time the design study was completed. Use of this laser resulted in the performance shown in Table 4. The compromise is primarily in the depth of penetration, but the performance obtained with the 15 kw peak power laser appears satisfactory.

2.1.3 Compromise System

Because the vegetation applications require two imaging bands (near infrared and red) and the water applications are best served with a pulsed laser, three active channels are needed to optimally satisfy all applications studied. Unfortunately, a three laser system, while feasible to build, would cost more than the contract could allow and would maximally tax the electrical power capabilities of the ERIM aircraft. Because the contract could not be augmented to provide the third laser channel, a decision was made to defer installation of the red band (0.64 μm) imaging capability and to provide a system with 1.06 μm imaging and 0.5-0.64 μm tunable profiling capability. Because the provision of special electronic circuitry for the topographic mapping capability also required additional contract funds which were not forthcoming, this capability was deferred also.

The impact of the compromises is that it will be difficult to map plant disease in lower canopy layers although the profiles, operating at 0.64 μm, provide some non-imaging support for this application.

The constructed system is, however, an experimental active-passive scanner, and provisions were made for the addition of other lasers

TABLE 3. SUMMARY OF SCANNER ACTIVE BAND PERFORMANCE REQUIREMENTS — WATER APPLICATIONS

Application	Required Information and Precision	Wavelength of Operation (μm)	Transmitted Pulse Width	Laser Power
Water Depth Mapping	Water Depth ± 1 ft (D), ± 2 ft (M) to 20 m in mean coastal water	0.51 - 0.58 μm	2.7 nsec (D) 5.4 nsec (M)	4.2×10^7 W
Sediment and Optical Properties Mapping	Scattering coefficient of 1 m layers ± 10% at S = 0.1-2.0/m coastal water to 4 m depth	0.51 - 0.58 μm	8.9 nsec	1.5×10^4 W
Rhodamine WT Dye Mapping	Concentration of Rhodamine WT±10% in 1 m thick water column at 5 μg/ℓ concentration in mean coastal water	0.546 μm excitation 0.565 - 0.615 μm receiver	8.9 nsec	2.15×10^4 W

D: desired

M: mandatory

TABLE 4. OBTAINABLE VERSUS DESIRED PERFORMANCE FOR WATER APPLICATIONS

Application	Desired Performance	Obtainable Performance*
Water Depth Mapping	Water Depth ± 1 ft (D), ± 2 ft (M) for water depths to 20 m	Water Depth ± 2 ft to to depths of 7 m
Sediment of Optical Properties Mapping	Scattering coefficient of 1 m layers ± 10% at S = 0.1-2.0/m in maximum coastal water	Required performance to 4 m depth
Rhodamine Wt Dye Mapping	Concentration of Rhodamine WT ± 10% in 1 m thick water column at 5μg/ℓ concentration in mean coastal water	Required performance achieved near water surface

* With 15 kw peak power nitrogen-laser-pumped dye laser

D: desired

M: mandatory

or capabilities with relatively little effort. Thus, a red band imager and/or topographic mapping capability can be added to the present system at minimum additional cost.

2.2 SYSTEM DESIGN PERFORMANCE

The AAFE active/passive multispectral scanner is essentially an expanded version of the M7 passive scanner [1] whereby two laser transmitters and receivers have been added at a sacrifice of two of the four passive detector positions. One addition provides active imagery at 1.06 μm and the other provides a profiling mode of operation at a (recording) limited rate of 8 pulses per second. Since the active data are to supplement the passive data, all 12 channels must have common registration and spatial resolution. Even the line trace profilometer must be correlatable with specific pixels in the imagery.

The M7 design parameters which are common with the passive portion of the AAFE scanner are listed in Table 5 with more detailed specifications of the active/passive system shown in Table 6. Primary system operation at ERIM was to be a 60 scans/sec although scanner operation at 100 scans/sec was to be a demonstrated capability. The higher scan rate provides contiguous scanning at a V/H = 0.2 but the resulting scanner data exceed the bandwidth capability of ERIM's airborne data recording equipment. This data recording function is not part of the active/passive scanner development. The scan lines are underlapped by 40% at 60 scans/sec, with a V/H of 0.2, but this is tolerable for operational testing of the system and for demonstrating system performance in selected applications.

System provisions for the profiling mode were not completed due to failure of the pulsed dye laser vendor to deliver an operable transmitting unit before contract completion. The transmit/receive optics, fast receiving detector, and pulse analyzing instrumentation however were provided. The eventual system capability is dependent upon delivery of an alternate dye laser unit.*

*A molectron dye laser has been incorporated in the scanner system, and satisfactory profiling operation has been verified in more recent flight operations.

TABLE 5. M7 SCANNER PERFORMANCE CHARACTERISTICS

12 Spectral Bands in UV, Vis. IR

90° External FOV ($\pm$ 45° from nadir)

2 mrad Max. Spatial Resolution, 3 mrad Nominal

0.1° C Nominal Thermal Resolution

1% Nominal Reflectance Resolution

5 Radiation Reference Ports

5 in. Diameter Collector Optics

60 or 100 scans/sec Scan Rate

DC to 90 KHz Electronic Bandwidth

Roll Stabilized Imagery

TABLE 6. AAFE SCANNER SPECIFICATION ACTIVE/PASSIVE EARTH RESOURCES SYSTEM

Parameter	Value
Laser Wavelength for Active Imagery	1.06 μm
Laser Wavelengths for Prolifometry	0.38 to 0.64 μm Tunable
Center Wavelengths for Passive Imagery	0.45 μm 0.48 μm 0.50 μm 0.52 μm 0.54 μm 0.57 μm 0.61 μm 0.65 μm 0.75 μm and 1.7 or 11.0
Field of View	90^{o}
Instantaneous FOV	2.0 mrad
Altitude	1000 ft (V/H = 0.2)
Ground Speed	200 ft /sec
Scan Speed	100 scans per sec. in Mode 1 60 scans per sec. in Mode 2
Signal Bandwidth (Video Amplifiers)	160 kHz in Mode 1 95 kHz in Mode 2
Type Tape Recording	M^2S Digital (HDDT)
Number of Recorded Tape Channels	12 Scanner Video 2 Auxilliary

The active/passive AAFE scanner system was designed to have a 2 mrad spatial resolution. This corresponds to a 2 mrad instantaneous field-of-view for the passive receivers and a 2 mrad beam divergence for the laser transmitters. The laser receivers however were designed to have a 3 mrad field-of-view to allow for alignment variations between the transmitter and receiver fields-of-view as a function of scan angle.

It was necessary to use two scanning mirrors, one to transmit and another to receive the active radiation in order to (1) eliminate atmospheric backscatter and (2) compensate for optical transmit time. At 1000 ft. altitude with a receiver area of 100 cm^2, the ground return is about 10^{-9} of the transmitted radiation. Backscattered radiation from the atmosphere below the aircraft, however, is on the order of 10^{-7} that of the transmitted beam and optical components which are common to both the transmit and receive beam, such as the single scan mirror, would scatter even more radiation into the receiver to significantly obscure the desired ground return. In addition, the finite travel time (about 2 μsec at 1000 ft. altitude) of the laser radiation to the ground and back requires a 0.75 mrad lead angle between transmitter and receiver beams in the direction of scan at nadir. The increasing travel time results in a gradual loss of registration as the system scans off nadir.

These two problems are most easily remedied by the use of two physically separated scan mirrors. Since the laser beam and receiver field-of-view intersect at a great distance from the scanner, $1/R^2$ attenuation of the scattered radiation makes it negligible. Lead time of the laser beam with respect to the receiver beam can be accounted for by an off-set of the two scan mirrors in the direction of mirror rotation (i.e., the laser mirror leads the active receiver mirror). However, a new problem, parallax, is introduced. With both scanning mirrors off-set slightly from 45^o, instead of a straight line scan on the ground, a slightly curved parabola will be followed. Since the curvature of the parabolas is

opposite for the laser beam versus the receiver beam, if they are well-centered at nadir then their centers will be misaligned as the angle deviates from nadir. Since the effect is small, it has been compensated for by using a receiver field of view of 3 mrad while maintaining a laser beam of 2 mrad. Thus, more than twice as much solar radiation is accepted by the detector, but use of a high power laser and a narrow bandpass filter at the detector keeps the solar background lower than the laser return by more than an order of magnitude. An illustration of receiver/transmitter tracking as a function of scan angle is Figure 3. Although the receiver field-of-view is 3 mrad, the active resolution element is defined by the 2 mrad laser beam and is consistent with the resolution of the rest of the scanner system. For most application, this 2 mrad (or 2 ft at 1000 ft) spot size on the ground is more than adequate, and smoothing or averaging of the data is possible to further improve the signal-to-noise ratio.

The key to the usefulness of the active and passive scanner data in various applications is the signal-to-noise performance. The passive band performance will not be discussed here since this system will duplicate the M7 design which has demonstrated adequate performance over the past five years of operation. The M7 performance is documented in Reference [1]. The design equivalent reflectance performance of the active scanner bands is presented in Table 7 along with a listing of parameters used in the calculations. For the 1.06 μm imaging channel, the received laser radiation is roughly an order of magnitude greater than for the solar radiation. In Section 2.3 where system performance is discussed, the fact that the solar radiation is indeed approximately an order of magnitude weaker than the laser return is verified.

The expected noise equivalent reflectance values are well within the mandatory requirements established in the applications discussion in Section 2.1. As mentioned in Section 2.1, for most applications, a further improvement in signal-to-noise can be achieved in processing the

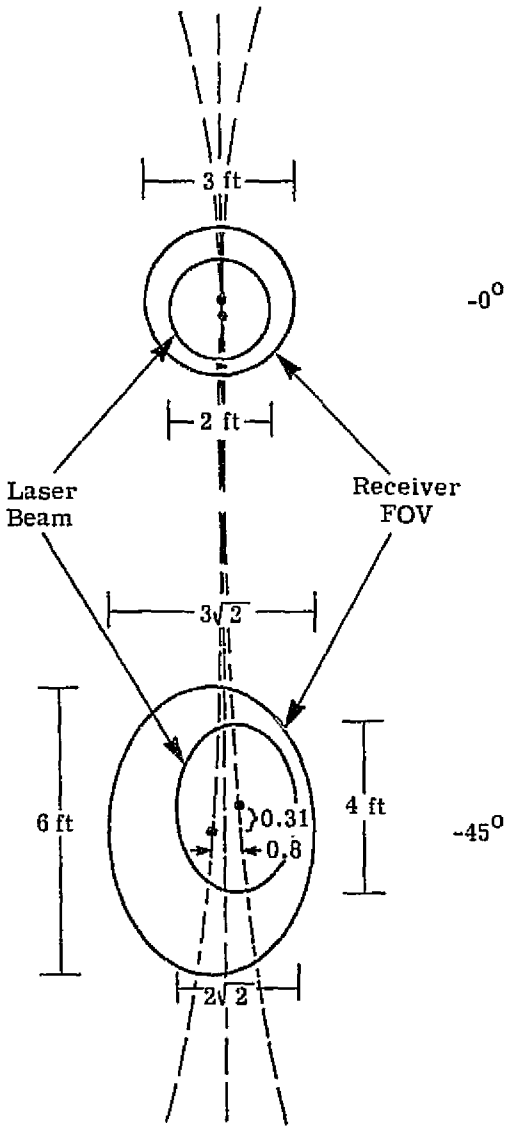

Operating altitude	1000 ft
Laser beam	2 mrad
Receiver field of view	3 mrad
Total scan field	±45°
Maximum range (at 45°)	1414 ft
Misalignment at 45°	0.414 mrad
Scan mirror separation	2 ft

FIGURE 3. TRANSMITTER RECEIVER MISALIGNMENT WITH SCAN ANGLE

TABLE 7. PERFORMANCE COMPUTATIONS

		Work Statement		Final	
		Imager	Profiler	Imager	Profiler
λ	*Laser Wavelength, μm	1.064	0.54	1.064	0.52**
P_L	*Laser Power, watts (peak)	30	15,000	30	18,000**
τ	Pulse Width, sec	CW	4E-9	CW	4.5E-9**
ε_t	Transmitter Efficiency	0.61	0.68	0.61	0.68
ε_c	Coupling Efficiency	0.95	0.95	0.95	0.95
ε_r	Receiver Efficiency	0.22	0.31	0.22	0.31
θ_t	*Transmitter Beam Divergence, rad	0.002	0.002	0.002	0.002
θ_r	*Receiver Beam Divergence, rad	0.003	0.003	0.003	0.003
ρ'	*Scene Reflectance, $ster^{-1}$	$0.26/\pi$	$0.05/\pi$	$0.26/\pi$	$0.05/\pi$
A_r	*Collecting Area, cm^2	106.4	106.4	106.4	106.4
r	Scan Rate, rev/sec	100	100	60**	60**
Θ	Scan Angle, deg. from nadir	0	0	0	0
$e^{-\tau \sec \Theta}$	Atmosph. Trans.	0.9287	0.8985	0.9287	0.8985

* Key Parameters

** Parameter Changes -- See Text (Section 2.4.3)

TABLE 7. PERFORMANCE COMPUTATIONS (Continued)

		Work Statement		Final	
		Imager	Profiler	Imager	Profiler
V	*Aircraft Vel., cm/sec	6096	6096	6096	6096
	ft/sec	200	200	200	200
H	*Aircraft Alt., cm	30,480	30,480	30,480	30,480
	ft	1000	1000	1000	1000
$E_{\lambda s}$	Solar Spectral Irradiance, watts cm^{-2} μm^{-1}	0.055	0.14	0.055	0.14
ϕ	Solar Elevation, deg.	45^{o}	45^{o}	45^{o}	45^{o}
L_P	Path Radiance, watts cm^{-2} μm^{-1} $ster^{-1}$	1.13E-4	6.39E-4	1.13E-4	6.39E-4
$\Delta\lambda$	Band Pass Filter Width, nm	2.5	1.2	5.5**	6.7**
R_a	Detector Sensitivity, amp/watt	0.25	0.053	0.25	0.053
G	Gain	$\sim$ 100	1.1E+5	$\sim$ 100	1.1E+5
NEP	Noise Equiv. Power, watts $hz^{-1/2}$	1E-13	---	1E-13	---
F	Noise Factor	3.98	1.284	3.98	1.284
e	Charge on Electron, coulombs	1.6E-19	1.6E-19	1.6E-19	1.6E-19

* Key Parameters

** Parameter Changes -- See Text (Section 2.4.3)

TABLE 7. PERFORMANCE COMPUTATIONS (Continued)

		Work Statement		Final	
		Imager	Profiler	Imager	Profiler
i_d	Detector Dark Current, amps	0	2E-11	0	2E-11
P_R	*Received Laser Power on Detector, watts	3.1E-8	5.4E-6	3.1E-8	5.3E-6**
P_S	*Solar Power on Detector, watts	1.6E-9	7.3E-10	3.5E-9	4.1E-9**
Δf	*Information Bandwidth, hz	157,100	175E+6	94,000**	175E+6
i_s	Signal Current, amps	7.8E-9	2.3E-7	7.8E-9	2.8E-7**
i_n	Noise Current, amps	4.2E-11	4.1E-9	4.2E-11	4.5E-9**
i_s/i_n	Signal-to-Noise Ratio (power)	14	8	14	9
$NE\Delta\rho$	*Noise Equivalent Reflectance, % (does not include noise modulation on the laser beam)	0.14	0.09	0.14	0.08
	Water Penetration, feet	--		--	24

* Key Parameters

** Parameter Changes -- See Text (Section 2.4.3)

TABLE 7. PERFORMANCE COMPUTATIONS (Continued)

$$P_R = \frac{P_L \rho' \varepsilon_t \varepsilon_c \varepsilon_r A_r \cos^3 \theta \, e^{-2\tau \sec \theta}}{H^2}$$

$$P_S = \Delta\lambda \varepsilon_r A_r \theta_r^2 \left(\rho' E_{\lambda s} \cos\phi \, e^{-\tau \sec \theta} + L_P\right)$$

$$i_s = R_a P_R$$

$$i_n = \left[R_a^2 NEP^2 \Delta f + 2eF \left\{R_a (P_s + P_L) + i_d\right\} \Delta f\right]^{1/2}$$

$$\Delta f = \frac{L}{2t_{dwell}} = \frac{\pi_r}{\theta_t}$$

$$NE\Delta\rho = \frac{\Pi\rho' \, i_n}{i_s}$$

data. For instance, in agricultural investigations a pixel element no smaller than 10 ft x 10 ft is preferred for smoothing over row crops and individual plants. Therefore, at 1000 ft altitude and 2 ft (2 mrad) resolution, data from this system can be averaged over 5 x 5 elements to provide a factor of 5 improvement in noise equivalent reflectance over that shown in the Table.

The predicted surface penetration and reflectance resolution of the pulsed laser system will allow the reflected return from both vegetation canopies and water depths up to 24 ft to be recorded for computer analysis of reflectance variations within the penetrated surface. Further, this penetration pixel is registered with pixels in imagery at other wavelengths, both active and passive.

The range resolution for surface penetration is expected to be about 1.5 ft in water. The resolution is very dependent upon the relative amplitude and sharpness of adjacent returns as well as the sharpness of the transmitted pulse. The transmitted pulse will be about 4.5 ft long in air and 3 ft in water. The range or absolute altitude determination resulting from the time measurement between the transmitted and received pulses will be accurate to about 10 ft for a flight altitude of 1000 ft. Again, the resolution of this measurement is very dependent upon the characteristics of the reflected pulse.

2.3 SYSTEM TEST PERFORMANCE

When the active/passive multispectral scanner was completely assembled, bench tested in the laboratory, and installed and checked out in the aircraft, it was ready for its airborne performance tests. Immediately preceding its first airborne test, the aircraft and scanner were positioned 1000 ft from a target range in order to operate the entire system and assure registration between all channels and verify the expected signal levels and resolution. (See Appendix A for bench test results.)

Figure 4 depicts the target range. A 4 x 8 foot black painted wooden panel was covered at its base with a 4 x 4 foot white painted wooden panel. At the top of the black panel was mounted a 2 x 2 foot piece of flame-sprayed aluminum (Lambertian, diffuse reflector; $\rho' \sim 1.0/\pi$ steradian^{-1}). The scanner in the aircraft was able to scan vertically through the target scene by use of a folding mirror mounted to the scanner frame. When oriented at 45^{o} this mirror would provide a scene at the scanner nadir (angles off 45^{o} could provide off-nadir scenes).

Preliminary alignment of the scanner was achieved by removing the passive infrared detector and dichroic mirror, and replacing it with a prealigned (during laboratory tests) cross hair, diffusing plate and image magnifier. This foresight allowed visual alignment of the scanner system to an accuracy of about 2 mrad.

It is emphasized that these ground tests at a 1000 foot range were essential to assure registration between the various receiver channels. Since the mirror separation on the scanner is 2 feet between centers, alignment may not easily and accurately be achieved in the laboratory (unless a long focal length 30 inch diameter parabolic reflector is available). The laser receivers at one end of the scanner must be aligned to both the transmitted laser beams and the passive receivers at the other end of the scanner. This was most readily achieved by providing a target at 1000 ft range under static conditions except for scanning.

All optical components in the scanner system were prealigned in the laboratory using several precision machined surfaces located throughout the scanner structure. This prealignment provided an alignment accuracy of a few mrad between the two separate ends of the scanner system. The complexity and sensitivity of the spectrometer alignment dictated it not be touched once it was aligned on the collimator bench. Fine alignment of the scanner system, therefore, revolved around the spectrometer and proceeded as follows:

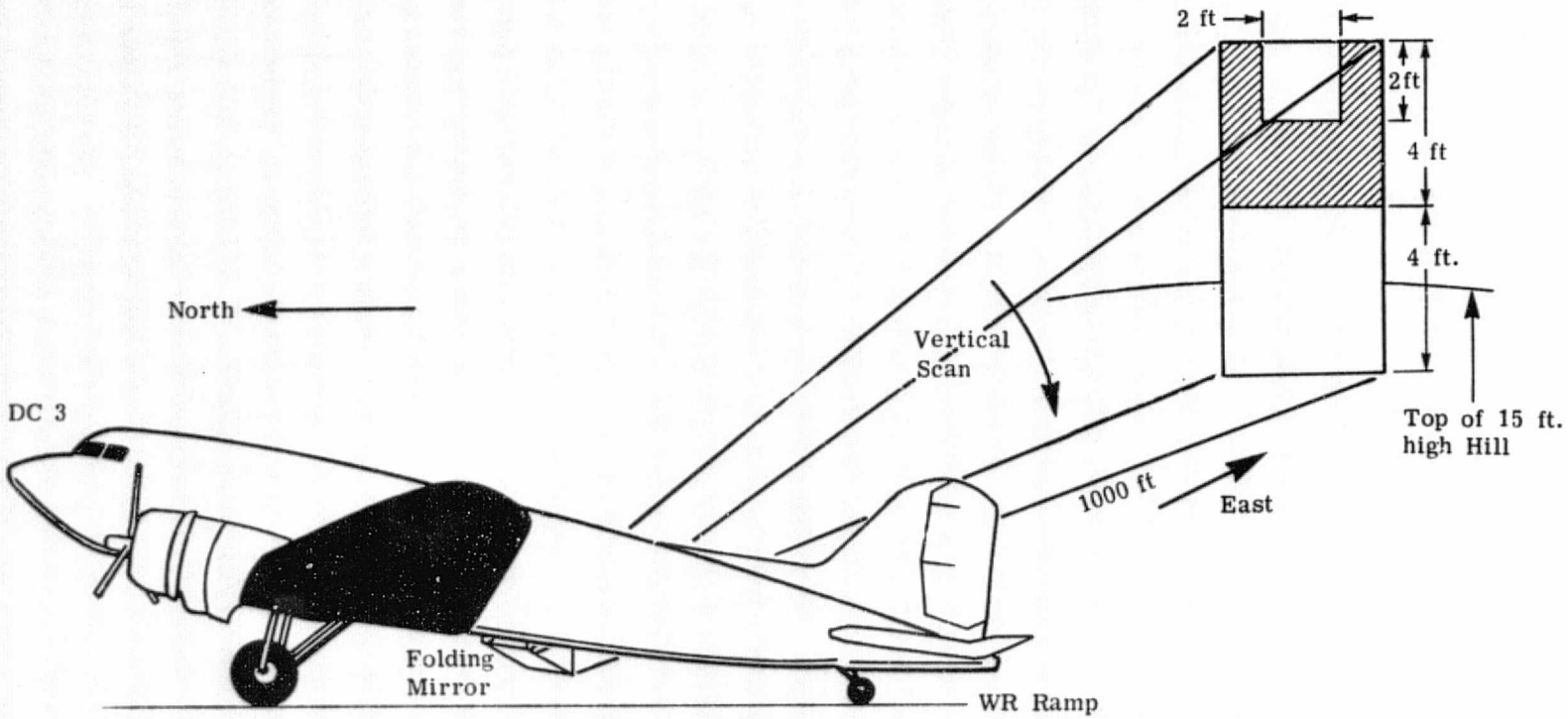

FIGURE 4. TARGET RANGE FOR AIRCRAFT RAMP TESTS

1. Obtain boresight of target -- static.
2. Move 45° mirror and/or target so that optimum spectrometer output is obtained -- dynamic.
3. Adjust IR detector to obtain registration with spectrometer.
4. Remove filter from active detector(s) and adjust aperture position to obtain near registration with spectrometer (passive receiver should lead active receiver by 2 μsec or 0.75 mrad* at 1000 ft).
5. Replace filter and adjust laser beam steering mirrors for maximum detector output and best target resolution.

Figure 5 shows A-scan oscilloscope traces of the target scene when scanning is done through the target panels top to bottom. From left to right on the trace are:

1. sky
2. flame sprayed aluminum, 2 ft
3. black panel, 2 ft
4. white panel, 4 ft
5. snow covered hill
6. snow covered foreground.

Detector labels are:

PMP -- PhotoMultiplier tube for reception of Pulsed laser return. (This detector was used passively in the broad visible region since the pulsed dye laser was not functional).

PMS -- Selected PhotoMultiplier tube on Spectrometer for reception of passive solar return.

LE -- General Electric Laser Eye SiAPD with 1.064 μm filter for reception of cw laser return.

Traces (a) and (b) show registration between the passive receiver and the active receiver end of the scanner. Traces (c) and (d) show registration

---

* Scan Mirror: 60 scans/sec = 120 π rad/sec = 0.12 π mrad/μsec

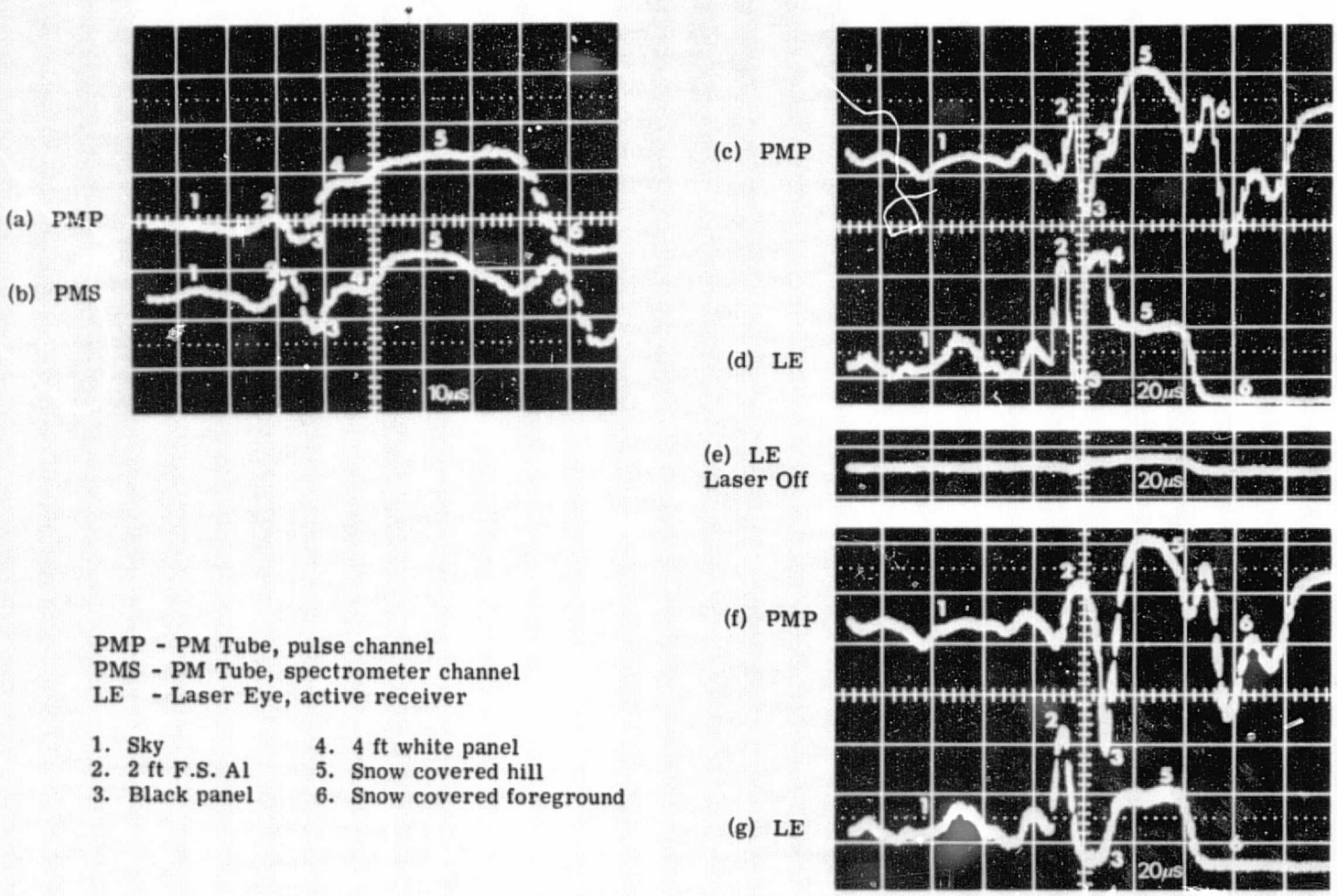

PMP - PM Tube, pulse channel
PMS - PM Tube, spectrometer channel
LE - Laser Eye, active receiver

1. Sky
2. 2 ft F.S. Al
3. Black panel
4. 4 ft white panel
5. Snow covered hill
6. Snow covered foreground

FIGURE 5. LINE SCANS OF TARGET SCENES WITH CALIBRATION PANELS

between the two active receivers and Trace (e) shows the Laser Eye output when the Nd:YAG laser was blocked and solar illumination of the snow covered hill provided a passive signal. It should be noted that the panels and hill were facing west and were well illuminated by a clear-sky, afternoon (about 2:00 p.m.) sun. Traces (f) and (g) show the same scene with the 4 ft white panel removed. In all traces, the 2 ft (2 mrad) flame-sprayed aluminum and 2 ft black panel are well resolved in both active and passive channels. All detectors can be seen to be in registration in the "direction of flight" (north) and in registration to within a single resolution element in the direction of scan.

It is emphasized that the ground tests are to provide only fine adjustment for the various transmitter and receiver beams to optimize the signal levels and assure mutual registration. Since the active and passive receiver telescopes were aligned in the laboratory using the machined reference surfaces, they were secured in position and no provision is (or should be) made for further operational adjustment. Only a small amount of fine adjustment of the detectors (and/or apertures) in the focal planes can be tolerated. During the ground tests, the active and passive receivers were in close enough registration that further fine adjustment was not necessary. Only the IR detector (which had been removed to accomodate the boresight optics) required fine adjustment, and the path of the Nd:YAG laser had to be changed by about 2 mrad in order to get the optimum signal return.

Immediately following the ground tests the system was flown in the ERIM DC3C aircraft at 1600 on 19 March 1977. The thermal detector (9-11.4 μm) was used in the IR channel, and 9 channels of the spectrometer were used to comprise the passive system. The Nd:YAG laser was operational and the 1.06 μ active receiver provided the active imagery. Since the pulsed laser was not included in the system, the active pulse receiver was operated passively without an optical filter. Data were taken over the Willow Run Airport Ramp for four separate passes at altitudes

of 950, 1000, and 1050 ft. Both active (1.06μm) and passive data were taken. On the fourth pass, the laser was turned off and the 1.06 μm active channel (Laser Eye) was used passively at an altitude of 1000 ft. Selected samples of the imagery appear in Figures 1 and 2.

Close examination of the active 1.06 μm imagery showed a good signal-to-noise ratio (see Figure 1). This was substantiated by examining the active 1.06 μm imagery when the laser was blocked. In order to use this channel to examine the solar leakage through the 1.064 μm, 55Å bandpass interference filter, it was necessary to increase the amplifier gain by a factor of 10. The resulting passive imagery, although much noisier than the active imagery, was still fairly good. This points out that the signal level of the laser return is adequate and that the active imagery has very good signal-to-noise performance. It also points out that the solar leakage at low sun angle in the daytime active imagery is less than one-tenth of the laser return signal when using a spectral filter with a 55 Å bandpass (in agreement with the calculations shown in in Table 7; compare P_R and P_S).

The uniformity of the active imagery denotes good laser operation. Previous experience with Nd:YAG laser imaging systems have shown gross non-uniformities in the imagery presumably due to low frequency amplitude fluctuations in the laser output. Although the amplitude noise of the CLC laser used on the active/passive multispectral scanner varies appreciably from day to day, it is not adversely affected by the severe thermal and mechanical perturbations found in an aircraft environment. The active imagery in this program was quite uniform and neither the presence of low or high frequency noise is evident. The day to day or slow variations in transmitted laser power are accounted for in calibrations provisions.

Nighttime data was taken using the same scanner configuration on 25 March 1977 at midnight. Active and passive (thermal) imagery of the airport ramp was taken for two passes, one at 1000 ft and the other

at 2000 ft. This imagery, along with imagery of downtown Ann Arbor at 1000 ft, also appears in Figures 1 and 2. The active imagery for both day and nighttime operation are identical in appearance except for the partial snow cover in the former case.

The 2000 ft data is particularly interesting since the system was designed for and aligned for a 1000 ft altitude. The alignment and amplifier gains for both runs were the same. The imagery is quite good at both altitudes even though the signal level would be expected to be down by a factor of about 3 due to parallax at 2000 ft and down by a factor of 4 due to $1/R^2$ attenuation. Resolution is, of course, still 2 mrad which corresponds to 4 ft on the ground at 2000 ft.

The night flight was not preceded by ground alignment checks, but it was preceded by three hours of flight time in which thermal imagery was taken. Analysis of that data showed that the thermal detector was operating with an NEΔT of 0.1° F. Figure 2c shows the airport ramp thermal imagery at 1000 ft altitude with an ambient ground temperature of 28°F.

The passive imagery presented in Figure 2 provides unobscured coverage of almost the entire 90 degree field-of-view of the scanner system. The active imagery in Figure 1, however, covers only about 60 degrees of scanner field-of-view. This is presumably due to loss of signal as a result of misregistration between the physically separated laser transmitter and the active receiver as the scan deviates significantly from nadir. In addition, minor optical misalignments and delays in the recording circuitry produced a skewness to the imagery. Both of these discrepancies should be easily corrected. In summary, the operation of the system and the quality of the resulting imagery was quite satisfactory for initial flight tests.

2.4 SYSTEM EQUIPMENT DESCRIPTION

Although various system configurations with differing capabilities were proposed for construction at the close of the design study, only a

minimal capability, basic system was authorized. The functions of this basic system are illustrated in the block diagram of Figure 6. Blocks 1 through 10 represent an existing passive scanner design to which active channels were added. The equipment of Block 1 was extensively modified to incorporate the changes. Otherwise, the new system was formed by adding to the old passive system equipment which was duplicated in the new system. The complete operable airborne system included some ERIM equipment in support of that developed for NASA. These system support functions are noted on the block diagram. The major system functions are described in the following sections.

2.4.1 Optical - Mechanical Scanner Configuration

The configuration of the Active/Passive Scanner was conceived as a modification and expansion of the already proven M7 Multispectral Scanner design. An optical schematic of the Active/Passive Scanner is shown in Figure 7. Essentially the scan mirror motor drives a single faceted mirror at each end of the motor's double ended shaft. A fixed folding mirror positioned immediately in front of one scan mirror is used to direct two laser beams onto the respective scan mirror. The other scan mirror is used to receive the laser signals after they have been reflected back to the scanner by surface objects. The two scan mirrors have been separated by a distance of 24 inches in order to preclude a retro return of a laser signal by near field atmospheric particulates. The two scan mirrors are slightly canted (1 mrad each) so that each mirror views a common object at an optimum range of 1000 ft while it is also torsionally displaced (1 mrad) so that compensation is achieved for time of transmission of each laser beam over a distance equal to double the range. The scan mirror drive is speed controlled using a motor-generator tachometer loop. For use in ERIM aircraft, the speed is nominally maintained at 3600 rpm. The system is, however, capable of operation to a maximum speed of 6000 rpm.

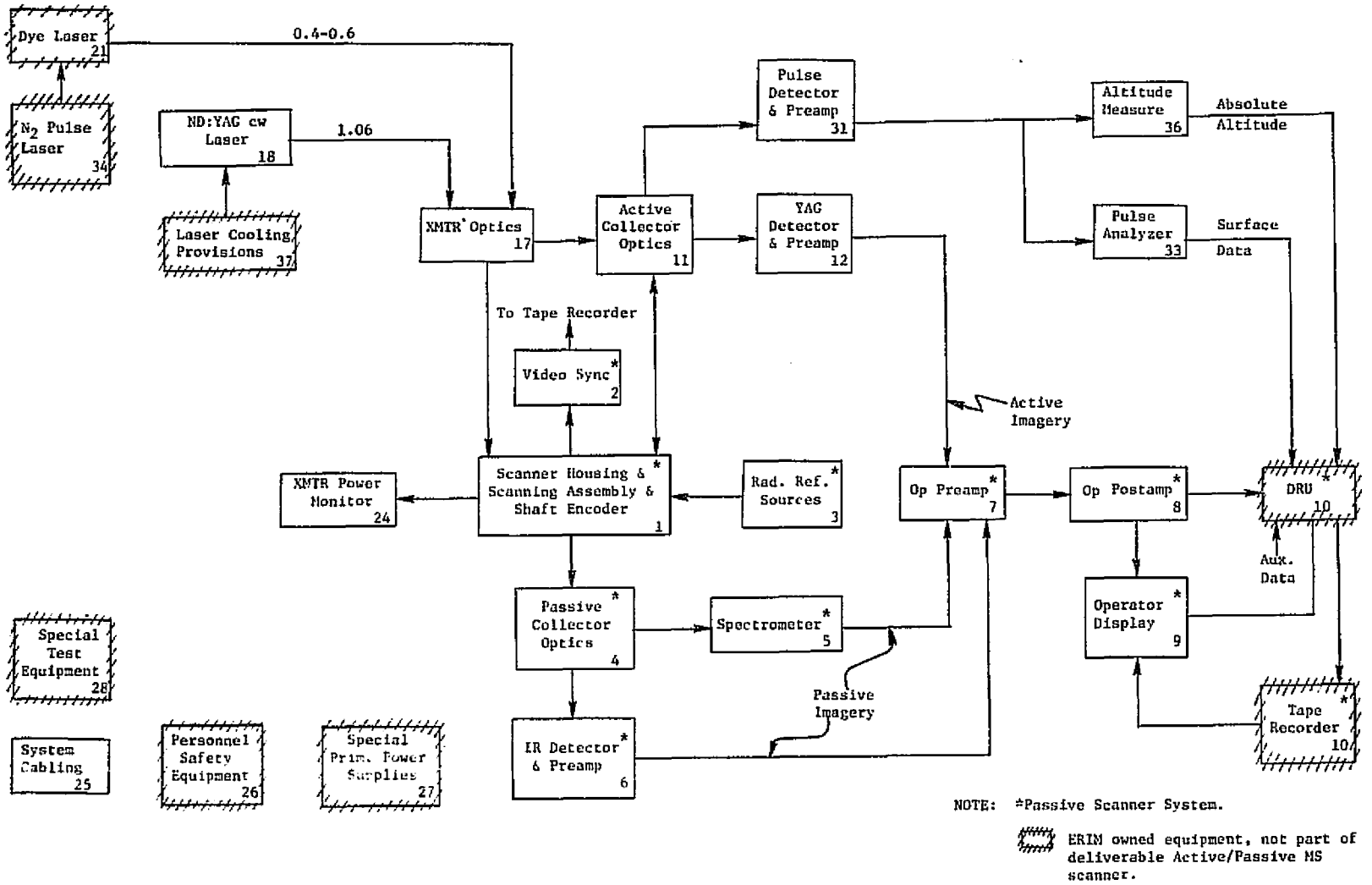

FIGURE 6. AIRBORNE ACTIVE/PASSIVE MULTISPECTRAL SCANNER SYSTEM

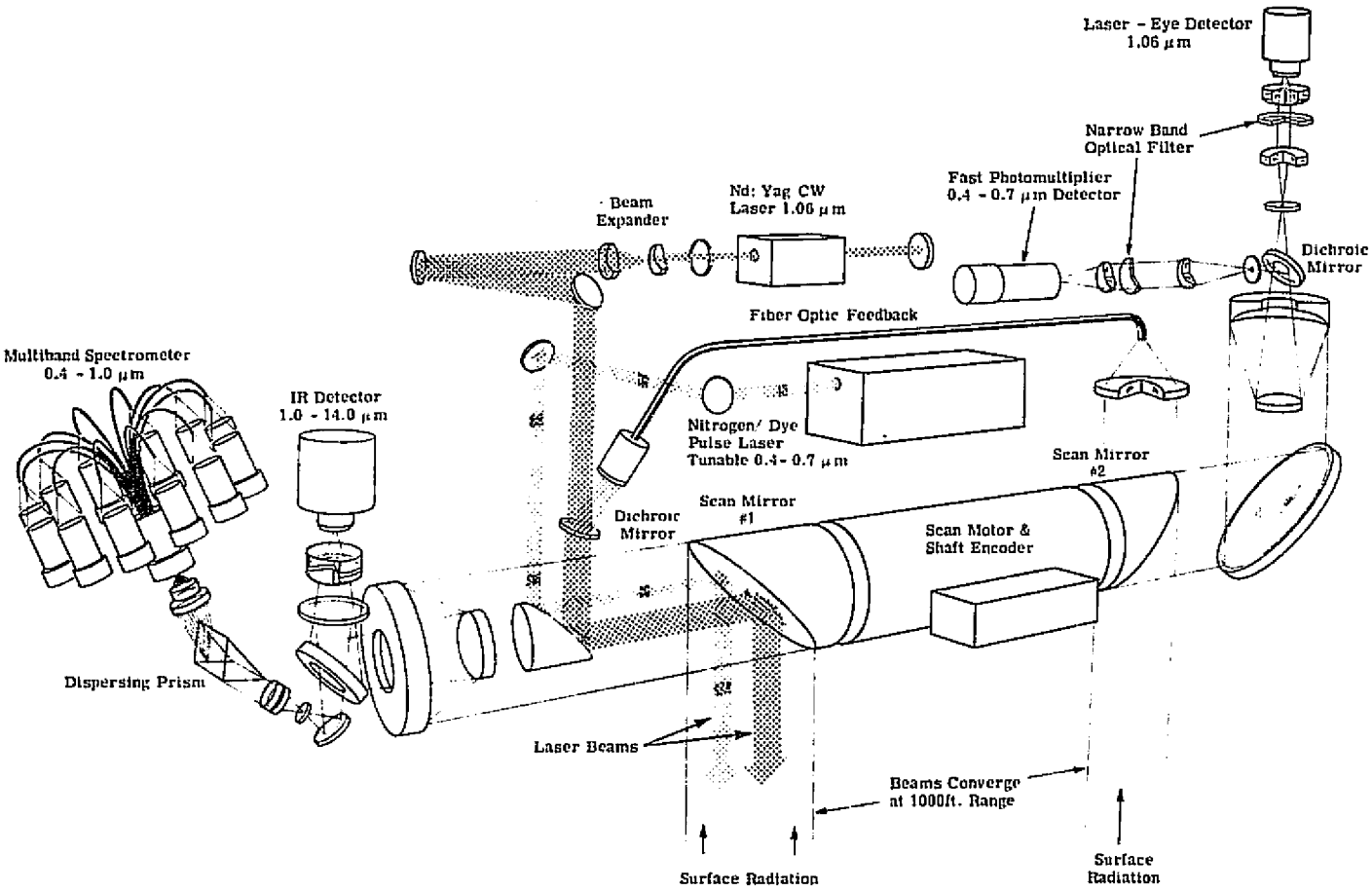

FIGURE 7. OPTICAL SCHEMATIC OF MULTISPECTRAL ACTIVE AND PASSIVE SCANNER

Two detector units are utilized to sense incoming passive radiation. These include a multichannel spectrometer and an infrared detector nominally filtered for operation in the 1.5 to 1.8 μm atmospheric window. The spectrometer, using a glass prism and photomultiplier detectors, can be configured to sense radiation in as many as 12 discrete wavebands in the range of 0.4 to 1.0 μm. The infrared detector(s) can be configured to cover any of a number of spectral bands in the range of 1.1 to 13.5 μm.

Two detectors at the opposite end of the scanner are utilized for receiving the retro reflected laser signals (Table 8). A photomultiplier is used to sense a return signal at laser wavelengths less than 0.68 μm while a silicon avalanche photodiode is used for wavelengths greater than 0.75 μm. Each detector is operated in conjunction with a narrow bandpass filter inserted in a collimated portion of the incident beam immediately ahead of each detector.

The entire assembly is rigidly designed to avoid deleterious distortions of any optical assembly. The entire unit shown in Figure 8 measures 98 inches long and weighs 750 pounds.

2.4.2 Passive Detectors and Calibration

The passive detector units which are part of the scanner assembly are a multichannel prism spectrometer and a filtered infrared detector. Photomultipliers with S20 or S1 photocathodes are the detector elements in the spectrometer. An InSb or HgCdTe detector flake cooled to liquid nitrogen temperature is the element for the separate infrared detector. A cooled filter, nominally selected for the 1.5-1.8 μm band, is used with the InSb detector for optimum signal-to-noise performance. An uncooled external filter is used with the HgCdTe detector for selected thermal bands between 3.5 and 13.5 μm.

While a choice of passive bands are available through spectrometer adjustments and detector filter selections, the intial configuration of the system provides the following:

violet	0.445 ± 0.035 μm
blue	0.475 ± 0.015 μm
blue green	0.500 ± 0.020 μm
green	0.520 ± 0.020 μm
green yellow	0.545 ± 0.025 μm
yellow	0.575 ± 0.025 μm
orange	0.610 ± 0.030 μm
red	0.660 ± 0.040 μm
infrared	0.805 ± 0.135 μm
infrared	1.65 ± 0.15 or 10.20 ± 1.20 μm.

For radiometric calibration of each passive band, once each line scan the detector views common radiation reference sources. These sources consist of a dark level, a point source calibration lamp and three full aperture, black body plates. The lamp brightness and the temperature of two of the plates are controlled by the equipment operator to approximate surface signals. The third plate is at ambient temperature. These integral sources are compared periodically with standards in the laboratory so that they provide known and acceptable calibration accuracy of the system at the instrument aperture.

The time history of a detector signal output during a line scan is shown in Figure 9. This trace as shown is the analog output of the detector with considerable dead time as the scanning aperture moves across different objects or radiation sources. This video signal may be recorded directly on tape in this analog form or it can be stored and sampled in digital form for more efficient tape recording.

2.4.3 Active Transmitters and Receivers

Imager -- CW Nd:YAG Laser Transmitter

A commercially available Nd:YAG laser unit was modified for airborne operation and was used in the near IR active channel of the scanner.

TABLE 8. ACTIVE RECEIVER PARAMETERS

A. Celestron Telescope (Collector Optics)

Type	Schmidt -- Cassegrain
Clear Aperture	5 inch diameter
Secondary Obstruction	2 inch diameter
Focal Length	50 inches
Speed	f/10

B. General Electric Laser Eye (Model 104)

Type	Silicon Avalanche Photodiode
Bandwidth	0.1 Hz - 1 MHz
Responsivity @ 1.06 μ	25 A/W
NEP/$\sqrt{Hz}$	4×10^{-4} W $Hz^{-1/2}$
Output Impedance	< 2000 ohms
Diameter	0.125 inches
Input Power	12.2 ± 0.2 vdc; < 150 ma
Avalanche Gain	100
Avalanche Voltage	2200 volts

C. RCA 8645 Photomultiplier Tube

Type	10-stage
Photocathode	S-20 multialkali
Maximum Voltage	1800 vdc
Maximum Average Anode Current	0.1 ma
Sensitivity (maximum)	0.064 a/w
Gain	0.11×10^6
Anode Dark Current	3 na
Anode Pulse Risetime	< 2 nsec

TABLE 8. ACTIVE RECEIVER PARAMETERS (Continued)

D. Filter Selection

Central Wavelength	Min. Peak Transmittance	Bandwidth
0.5179 μm	66%	0.0067 μm
0.5260 μm	84%	0.0084 μm
0.5380 μm	62%	0.0101 μm
0.5464 μm	61%	0.0108 μm
0.6328 μm	60%	0.0100 μm
0.6519 μm	64%	0.0114 μm
1.0644 μm	50%	0.0055 μm

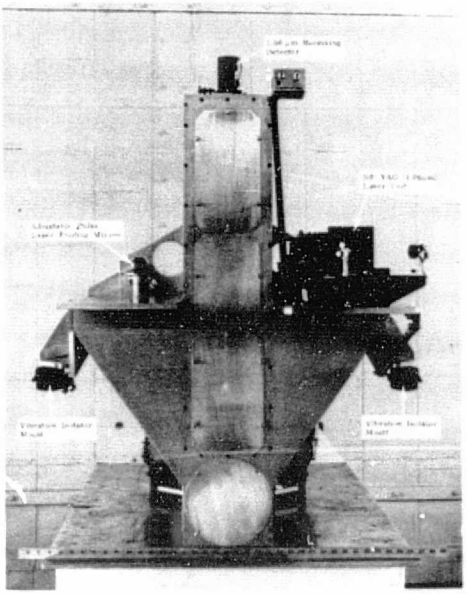

End View

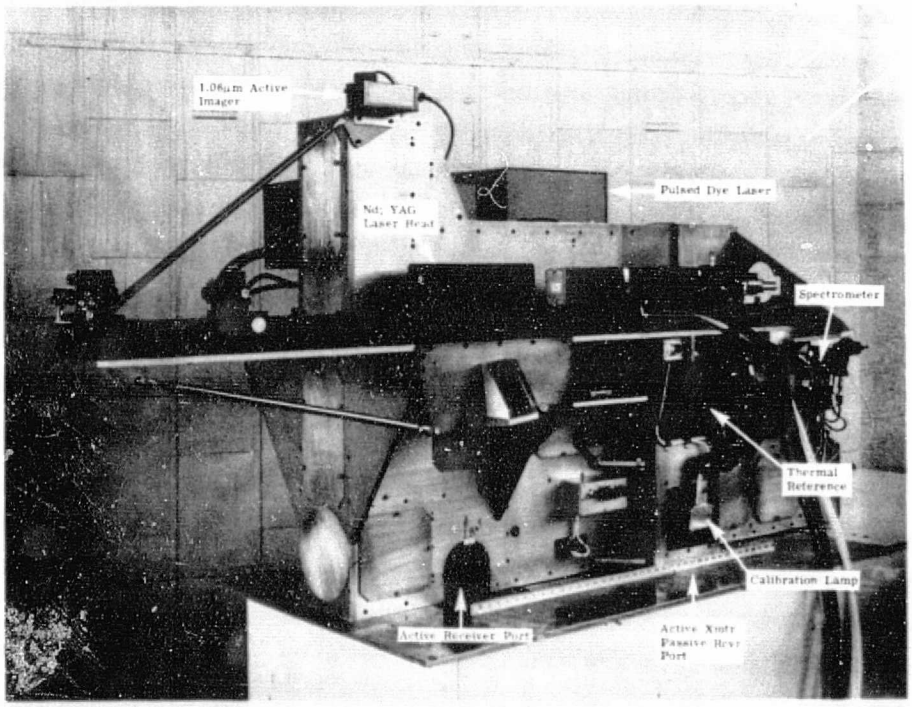

Side View

FIGURE 8. PHOTOGRAPHS OF ACTIVE/PASSIVE MULTISPECTRAL SCANNER

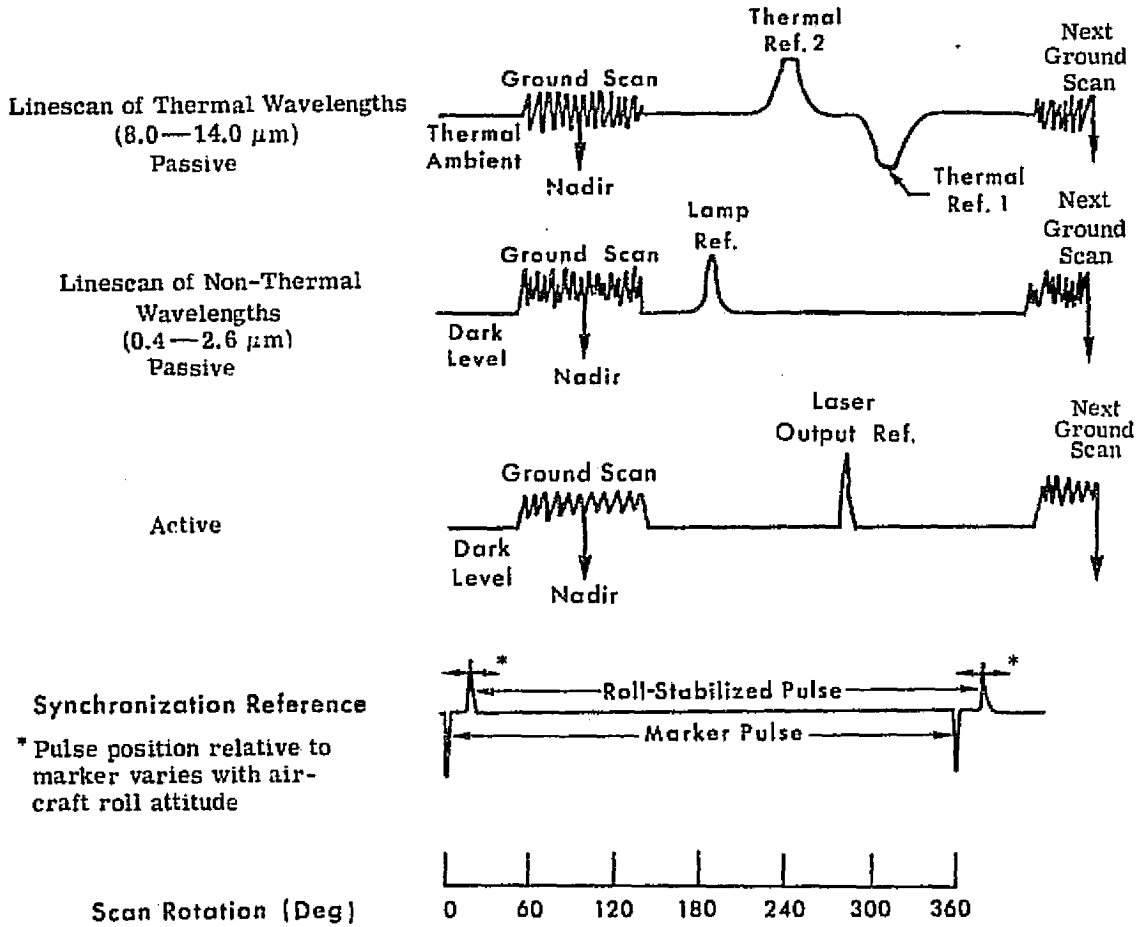

FIGURE 9. SCANNER VOLTAGE OUTPUT VERSUS TIME FOR IMAGERY

This Nd:YAG laser provides continuous wave (CW) radiation at 1.064 μm for two-dimensional active imagery of the ground scene. The laser parameters and a schematic of the laser assembly are shown in Figure 10.

The laser is comprised of a krypton arc lamp pumped Nd:YAG crystal designed for continuous high power operation. The laser is designed for operation in the TEM_{01*} or donut mode although TEM_{00} operation may be obtained by insertion of a limiting aperture within the laser resonant cavity, or multimode high average power operation may be obtained by shortening the laser cavity. The laser cavity is formed by two flat mirrors, one which is nearly 100% reflecting and one which is 90% reflecting, the latter being the output or coupling mirror. Maximum stable laser output is attained by critically aligning the laser resonating mirrors with the laser rod axis for the optimum (not necessarily maximum) lamp current.

The high pressure DC krypton lamp lies parallel to the Nd:YAG laser rod within an elliptical cavity to provide uniform optical pumping of the laser rod. Deionized water flowing over the laser rod and arc lamps forms the primary cooling system. Thermal energy is transferred from the primary cooling system to a secondary system of either tap water for laboratory use or an external cooling unit for flight operation. Since commercially available Nd:YAG lasers are designed for tap water cooling and 60 Hz operation, the laser system was modified for airborne cooling (radiator heat exchanger and refrigeration unit) and 400 Hz operation. Silicon controlled rectifier (SCR) switching is conventionally used for current regulation in most Nd:YAG laser systems and can lead to radio frequency interference (RFI) problems. An alternative regulation scheme using a transistor passbank does not have the electrical spiking found with SCRs. An argon laser power supply utilizing transistor current regulation was used to drive the Nd:YAG laser arc lamps and was provided as a special order by the laser manufacturer.

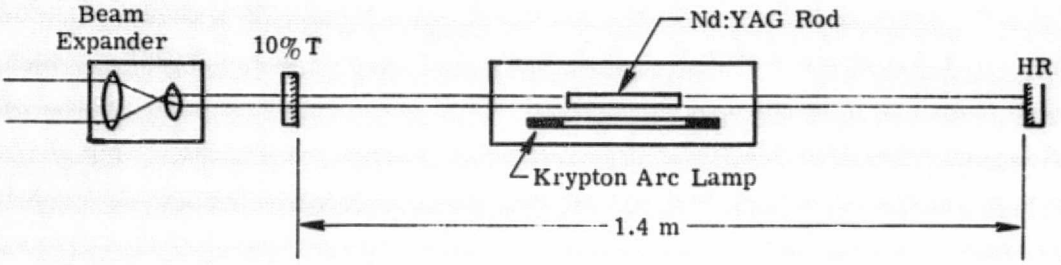

DC Krypton arc lamp 3.5 Kw
(160 vdc, 22 amps (max))
Elliptical pump cavity
Water cooled flooded cavity (deionized water)

	Donut TEM_{01}*	Gausian TEM_{00}	Multi-Mode
Power output	30 W	10 W	50 W
Beam diameter	2 mm	1 mm	4 mm
Beam Divergence (full angle)	2 mr	1 mr	9 mr

FIGURE 10. Nd: YAG LASER SYSTEM - CW OPERATION
(Schematic and Performance)

The lowest order TEM_{00} or Gaussian mode of the Nd:YAG laser can be obtained with an intra-cavity aperture to provide a laser beam about 1.0 mm in diameter with a diffraction limited divergence of about 1 mrad. The power output is about 10 watts in this low order mode and the beam is spatially stable with amplitude fluctuations at a minimum. Increasing the aperture size allows TEM_{01*} or donut mode operation with a corresponding increase in output power to about 30 watts but at the expense of greater beam size, greater divergence and greater amplitude fluctuations and spatial noise. Removal of the aperture and shortening of the laser cavity produces multi-mode operation with output power in excess of 50 watts, a beam size of several millimeters and a divergence of several mrad. Spatial noise is significant in this configuration due to the blinking on and off of the various transverse modes as they compete with one another.

In order to maximize the signal-to-noise (S/N) ratio of the active imagery, it is desirable to have as great a laser output power as possible without introducing excess laser noise. Quantitative noise values of the various laser modes are not available, but it is felt that the TEM_{01*} or donut mode provides the optimum output power and noise values for the active system. In applications requiring greater range, the laser can be operated in the high power multimode configuration. Similarly if an application dictates uniform (Gaussian) beamshape and can tolerate lower laser power, the Nd:YAG laser can be operated in the TEM_{00} mode.

A laser is essentially an optically resonant cavity with tolerances which are on the order of a wavelength of light. In order to maintain the laser output in a particular laser mode with a minimum of amplitude noise, the laser must be free of high amplitude mechanical perturbations. In an aircraft, this necessitates isolation of the entire scanner from the aircraft vibration and also requires a well balanced vibration-free scanner mirror and drive. This is particularly important for Nd:YAG lasers where acoustics and thermal perturbations can set up relaxation

oscillations in the laser rod. These oscillations are high amplitude and are on the order of 10^4 Hz, well within the information bandwidth of the scanner system.

This particular Nd:YAG laser was built by Control Laser Corp. of Orlando, Florida. It consists of a 4 x 75 mm Nd:YAG rod with 0.6 percent doping, and concave end faces having a 2 m radius of curvature. The system was designed specifically for long laser cavity, donut mode operation; although Gaussian or multimode operation is also easily achieved. The delivered unit employed flat dielectric coated mirrors separated by 1.5 meters to form the optical cavity. The laser head was located at the center of the cavity, and an aperture near the high reflectivity mirror was used for mode control. Dust covers between mirrors and laser head were provided to protect the optical surfaces from dust and damage.

Cooling of the high power, high pressure arc lamps and laser rod was achieved by passing water over these components. Since the electrodes are in direct contact with the water, it must be deionized to prevent current flow and resulting pitting of the gold coated elliptical pump cavity. A conductivity between 2 and 0.2 μmho/cm (0.5 to 5 MΩ · cm) was maintained at all times during the operation of the laser. Flows between 3 and 4 gallons per minute were used and a water temperature of 95° was maintained. Heat was removed from this cooling water through heat exchangers. These heat exchangers were coupled into secondary coolant loops which included a large radiator in the aircraft slipstream and a refrigeration unit in the aircraft.

Good stable donut mode operation was difficult to achieve using the delivered configuration. The donut mode was extremely sensitive to drive current and would often break up into multimode operation. In addition, relaxation oscillations were present and would completely dominate the laser output if an electric motor or power drill was placed in contact with the optical bench. This was corrected by going to a slightly shorter (1.4 m) and slightly asymmetric cavity such that no relaxation

oscillations could be found in the output and the donut mode could be maintained indefinitely.

Alignment of the Nd:YAG laser was achieved with a HeNe laser mounted to the Nd:YAG laser optical rail. The HeNe beam was also used to follow the path through the scanner system and to provide preliminary system alignment.

The 6x beam expander was used to increase the beam size of the intense laser output and therefore reduce its power density. This reduces the chances of damage to the mirror surfaces and reduces thermal heating effects which can warp the mirror. In addition, local fluctuations in the reflectivity of the scan mirror surface are averaged when a large portion of the scan mirror is used.

Imager -- SiAPD Receiver

The heart of the imaging laser receiver is the silicon avalanche photodiode detector which gives the best signal to noise (S/N) ratio for this spectral region (1.06 μm), signal level, and electronic bandwidth (90 and 160 kHz). The unit is made by General Electric and is designated Laser Eye (Model 104). This detector assembly shares, via dichroic beam splitter, the aperture of the active receiver collector optics with the profiler detector assembly. Each of these detector assemblies include narrow spectral band optical filters which minimize solar illumination of the scene. Solar radiation represents optical "noise" in the active imagery which is calibrated in terms of scene reflectance. These spectrally narrow optical filters require collimation of the radiation imposed upon them. Therefore, the active receivers include collimating and focusing lenses as well as the optical filters and radiation detectors.

The conventional narrow band (55 Å) interference filtering of the 1.06 μm detector provides an adequate laser-to-solar signal ratio of about 9 at the detector. The detector converts the radiation signal

to electron flow or current which is multiplied by an avalanche phenomena which is similar to that in a photomultiplier tube. This signal current is amplified for tape recording by conventional operational amplifiers. Once each line scan (during the internal scan view), a portion of the laser transmitted radiation is directed into the receiver using a 0.2% beam sampler and a fiber optic bundle (Fig. 7). This monitoring of laser transmitted power is required for reflectance calibration. Further discussion of reflectance calibration provisions for the active bands is presented in Appendix B.

Profiler -- Pulsed Dye Laser Transmitter

A commercially available nitrogen laser pumped dye laser was to be used as the active profiler transmitter for providing surface penetration data in various applications. The high peak power and tunable wavelength output of pulsed dye lasers was attractive and the short pulse duration of the nitrogen laser pumped system led to that choice. The Laser Energy Inc. Model 337 dye laser was chosen on the basis of short (less than 4 nsec), high peak power (15 kw) laser pulses and 400 Hz prime power capability. Laser Energy Inc., however, was unable (in a period of one year) to provide a useable laser even at reduced specifications (5 nsec, 10 kw). The profiler was, therefore, not functional in the active/passive multispectral scanner during acceptance testing of this system. An alternate system, the Molectron Spectroscan 10, was purchased at ERIM expense but did not arrive until after completion of the contract period. Work is progressing under a Navy contract to incorporate this new nitrogen laser pumped dye laser into the active/passive scanner system.

The Molectron nitrogen laser pumped dye laser system is basically the same as the Laser Energy Inc. system. Both employ nitrogen lasers which optically pump dye laser cavities and the dye laser outputs are similar in peak power, beam size and divergence. The principle difference lies in the pumping geometries of the two systems. Table 9 tabulates the specified parameters of the proposed system (Laser Energy) and the system presently being used (Molectron).

TABLE 9. NITROGEN LASER PUMPED DYE LASERS

	NITROGEN LASER	
	Laser Energy*	Molectron
Wavelength	0.3371 m	0.3371 m
Discharge	Longitudinal	Transverse
N_2 Gas	Sealed	Flowing (vacuum pump; gas bottle)
Beam Quality	Collimated	Divergent
Size	3 mm (diameter)	1.5 x 25 mm
Divergence	3 mrad	1.6 x 14 mrad
Pulse Width	9 nsec	9 nsec

	Dye Laser	
	Laser Energy*	Molectron
Wavelength	0.36-0.74 m	0.36-0.74 m
Optical Pump	Longitudinal	Transverse
Tuning	Prism	Grating
Linewidth	3 nm	0.3 nm
Pulse Width	4 nsec	4.5 nsec
Beam Diameter	1 mm	0.6 mm
Beam Divergence	1 mrad	4 mrad
Maximum Peak Power	15 kw	20 kw
Total Weight		100 lbs
Total Size		37 x 15 x 9 in.
Power Requirement		115 vac, 8A
Price	$9 K	$13 K

* Company failed to provide a workable system.

The scanner performance computations presented in Section 2 reflect minor changes in performance as a consequence of the different pulsed laser system (see Table 7). As may be seen from Figure 11, the Molectron laser output may be enhanced by going to wavelengths less than 0.54 μm. Although coastal water transmission is maximum at about 0.54 μm, only a small decrease in transmission is encountered by going to slightly shorter wavelengths. At 0.52 μm, water transmission has deteriorated by only a few percent while laser peak power output of the Molectron laser has gone from 10 kw to about 18 kw. This latter power level results in a slightly increased laser return signal over that presented in the work statement, and a corresponding decrease in the noise equivalent reflectance value. It should be noted that the active visible wavelength receiver has a broader bandwidth optical filter than was presented in the contract work statement, allowing a factor of 5 more background solar radiation to be incident on the detector.

The instrument, of course, is quite flexible with wavelength tunability throughout the visible spectrum. In addition, the nitrogen laser may be used by itself to obtain higher peak powers of about 50 kw at 0.3371 μm in the near UV for possible fluorescence experiments.

The nitrogen/dye laser unit pulses on command from a trigger pulse indexed into the ground scan of scanner imagery data channels. The pulse may be indexed anywhere in the scanner external field of view but cannot be repeated more often than once each 12 scan lines. This rate restriction results from the store and sample rates of the receiver pulse analyzer.

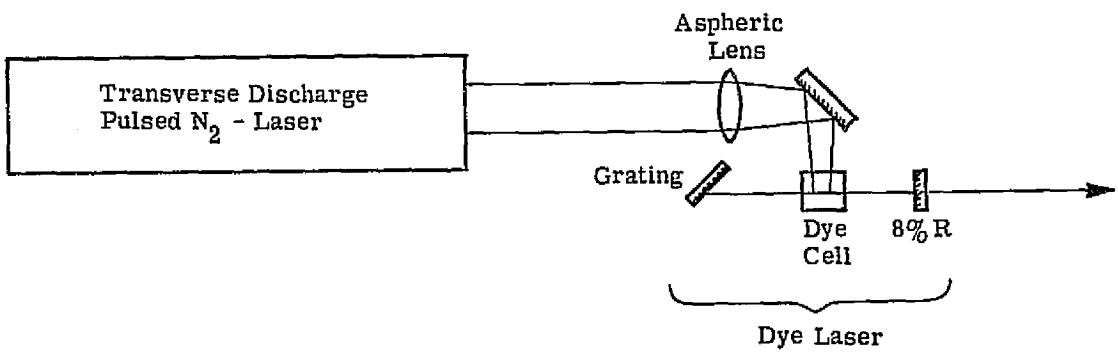

FIGURE 11(a). SCHEMATIC OF MOLECTRON SPECTROSCAN 10 NITROGEN LASER PUMPED DYE LASER

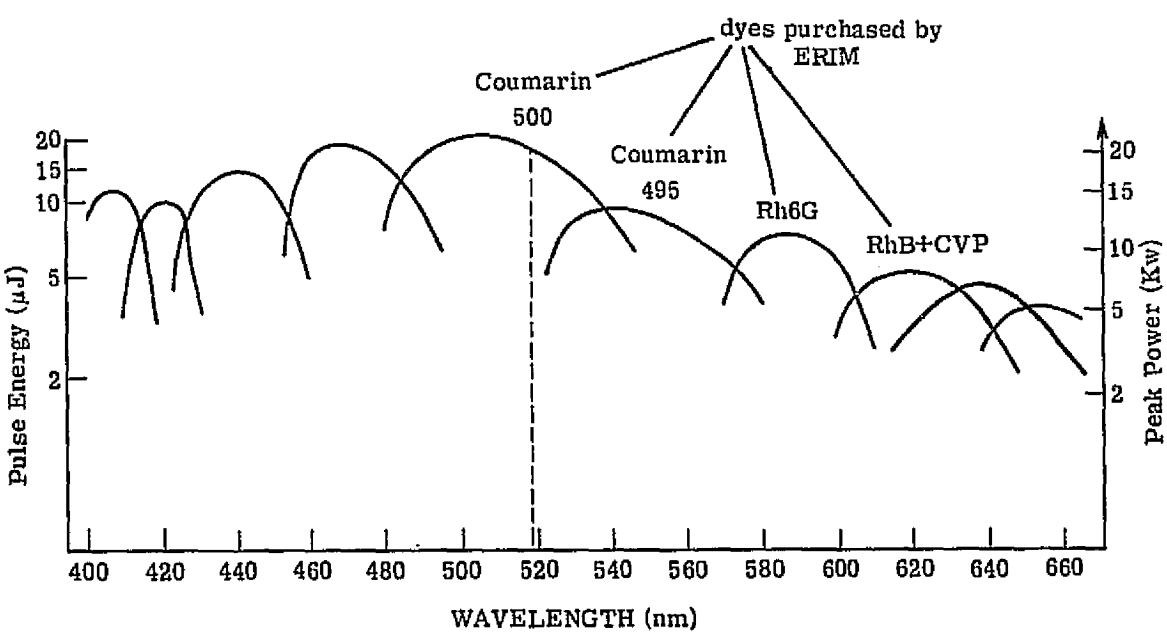

FIGURE 11(b). TUNABLE OUTPUT OF THE MOLECTRON SPECTROSCAN 10.

Profiler -- High Speed Photomultiplier Tube

In order to operate the scanner in its profiling mode for obtaining height or depth information, the short (tens of nanoseconds) dye laser pulse returns must be temporally resolved by the receiver. The fast response, low noise and high gain of a photomultiplier tube make it an ideal choice as the pulse detector. Several different PM tubes were considered, and the RCA 8645 with an S-20 surface and a rise time of less than 2 nsec was chosen. Although several other PM tubes possessed faster response time and/or greater quantum efficiency, they were all experimental tubes of questionable reliability. The RCA 8645 was chosen based upon extensive past experience with this detector, its rugged packaging, good shielding, good availability and low cost. Table 8 lists the specifications and operating parameters of this device.

Both the active profiler and the active imager use the same Celestron Schmidt - Cassegrain receiver telescope (see Figure 7 and Table 8). A "cold mirror" whose reflectance is greater than 90% in the visible spectrum (0.42-0.67 μm) and whose transmittance is greater than 85% in the near IR (0.75-2.5 μm) is used to direct the profiler radiation (visible) to the photomultiplier tube and yet allow the active imaging radiation (1.06 μm) to pass through to the Laser Eye Si APD detector. Immediately following the "cold" mirror and located near the telescope focal plane are respective adjustable apertures of 0.15 inch diameter which provide an instantaneous field of view of 3 mrad. The radiation is then collimated by a 4-inch focal length lens (6 inch lens for 1.06 μm channel) in order to accommodate a narrow spectral bandpass interference filter (and other filters such as a polarizer, if desired). The radiation is then reimaged onto the detector using a 4-inch focal length lens.

It should be noted that the broad electrical bandwidth (175 MHz) required to provide a temporal resolution of 2 nsec, limits the system sensitivity appreciably. Since noise current is proportional to the

square root of the electrical bandwidth, a strong signal level is re- to produce an adequate signal-to-noise ratio. This dictates laser transmitter power levels in the kilowatt range. In this system, the transient digitizer in the pulse receiver electronics limits the pulse (or sampling) rate to once each 12 scan lines (or 5 per sec at 60 scans/ sec).

Laser Safety Considerations

Calculations have been made using the American National Standard Institute (ANSI Z136.1-1976) maximum permissible exposure (MPE) levels to laser radiation. The results show the minimum operating ranges which can be used safely without danger to unprotected observers. The calculations are based on the performance numbers expected from the active system and do not allow for atmospheric lensing, beam focusing or other abnormalities which can occur.

Performance numbers used are given in the list below.

	1.06 μm	0.4-0.7 μm
Resolution (α)	2×10^{-3} mrad	2×10^{-3} mrad
Scan Dwell Time (τ)	5.3 μsec	4.5 nsec
Non-Scan Dwell Time (τ_1) @ 1000 ft. alt.	0.01 sec	4.5 nsec
Maximum Pk Power	20 W	10^4 W
A/C Velocity (V)	200 ft/sec	200 ft/sec

Assuming direct intrabeam viewing,

$$\text{MPE @ } 1.06\ \mu m = 5 \times 10^{-6}\ J/cm^2 \text{ for } \tau < 10^{-5} \text{ sec}$$

$$= 9\ \tau^{3/4} \times 10^{-3}\ J/cm^2 \text{ for } \tau > 5 \times 10^{-5} \text{ sec}$$

$$\text{MPE @ } 0.4 - 0.7\ \mu m = 5 \times 10^{-7}\ J/cm^2 \text{ for } \tau < 1.8 \times 10^{-5} \text{ sec}$$

$$= 1.8\ \tau^{3/4} \times 10^{-3}\ J/cm^2 \text{ for } \tau > 1.8 \times 10^{-5} \text{ sec}$$

NOTE: All of the above MPE's are for maximum night aperture of 7 mm which is the worst case level.

The exposure level can be determined by the following expression

$$\text{Exposure} = \frac{P_{PK}\ \tau}{\frac{\pi}{4}(\alpha R)^2}$$

from which the minimum operating range can be determined by inserting the MPE to give

$$R_{min} = \left[\frac{\frac{4}{\pi} P_{PK}\ \tau}{\alpha^2\ MPE}\right]^{1/2}$$

Substitutions in the range equation gives minimum safe operation ranges for both wavelengths with scanner mirror operating and stationary.

$$R_{min}(1.06)\text{scan} = \left[\frac{\frac{4}{\pi} 20(5.3 \times 10^{-6})}{(4 \times 10^{-6})(5 \times 10^{-6})}\right]^{1/2} = 25.9 \text{ m}$$

$$R_{min}(1.06)\text{non-scan} = \left[\frac{\frac{4}{\pi} 20 \times 10^{-2}}{(4 \times 10^{-6})(9)(\tau^{3/4})(10^{-3})}\right]^{1/2} = 148 \text{ m}$$

$$R_{min}(0.4\text{-}0.7)\text{scan} = \left[\frac{\frac{4}{\pi}(10^4)(4.5 \times 10^{-9})}{(4 \times 10^{-6})(5 \times 10^{-7})}\right]^{1/2} = 54 \text{ m}$$

These results indicate that a minimum aircraft altitude for equipment to be energized of say 500 ft must be specified as "standard operating procedure." At this altitude a range safety factor of at least three is achieved even when the scanner is not rotating.

2.4.4 Signal Handling and Recording

The analog signals from the scanner detectors are amplified in a series of preamplifiers at the scanner and postamplifiers at the operator console to bring the levels up to 3 volts for display and recording. The operator has manual control of the amplification. He monitors the 12 scanner data channels in analog form, 3 channels at a time on an oscilloscope. On the oscilloscope, time is displayed along the x-axis and signal amplitude as a y-axis deflection. The operator can view the scanner signals in analog form as both inputs and outputs to and from the tape machine. Therefore, satisfactory tape recording of the signals can be verified at the time of recording.

To obtain the best quality of signal recording and to use the magnetic tape most efficiently, the analog signals are digitized and rearranged in time before recording. Each video data channel is recorded on a separate tape channel in an 8-bit high density digital tape (HDDT) format. Thus, 256 discrete signal levels are recorded. The data format is a copy of the one established by Bendix for their M^2S multispectral scanner system. It provides for the recording of reference data along with the scanner video. The computer processing centers at ERIM, Bendix and NASA/JSC can retrieve the data directly in this format.

Special signal handling provisions were necessary to record all of the desired information in the active scanner channel using pulse transmissions. The desired information was contained in the total time history

of the signal amplitude, including both the transmitted pulse and its reflected return as illustrated in Figure 12. The time period T_H is convertible to the aircraft absolute altitude and the range of the optical transmission. Increments of the time period T_B represent the depth of surface penetration. The signal amplitude during the time period T_B represents the reflectance at a particular depth when it is compared with the amplitude of the transmitted pulse.

A commercial electronic unit called a transient digitizer (Model 7912) by its manufacturer, Tektronix, provides the necessary signal handling functions. It functions as a very high speed storage oscilloscope with a capability to digitize the acquired waveform and store it in a semiconductor memory. The stored waveform is then read into two channels of the HDDT tape recording. Since the readout is 512 x-y locations (10-bit data), it must be reformatted before it can be recorded on the 8-bit tracks for normal scanner video. Two 8-bit tracks are required for total information recording and, because of the digitization and readout time required, the pulse history can be recorded only once each 12 scan lines at 60 scans per second.

The transient digitizer was modified to provide a coarse time scale for time period (T_H) representing the optical range and a fine time scale for period (T_B) representing the depth of surface penetration. Thus, range to the surface can be determined to a resolution of about 10 ft and surface penetration to about 1 ft. The amplitude of the transmitted pulse is not directly represented in the stored pulse history because of its large amplitude compared to the reflected signal. However, it is registered in the proper position for time measurement and its recorded amplitude is indicative of the transmitted power.

2.4.5 System Installation in Aircraft

The system was installed in ERIM's DC3C aircraft for flight test before delivery and for flight operations after delivery. ERIM's aircraft had been previously modified to provide two large instrument wells

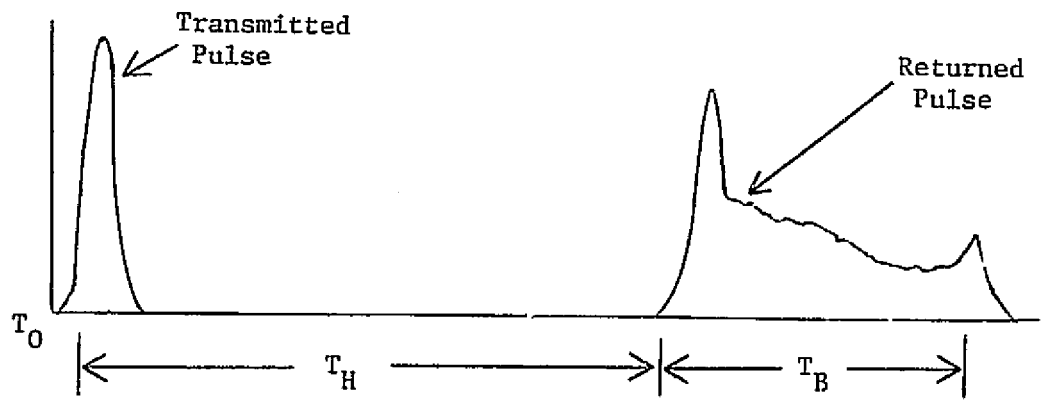

Figure 12. PULSE WAVEFORM AND MEASURED PARAMETERS

(each 2 ft wide x 6 ft long) through the floor near the rear of the aircraft and a 30 KVA 400 Hz turbine driven electrical power unit for airborne testing of developmental instrumentation systems.

The active/passive scanner assembly fills the starboard side instrument well as shown in Figure 13 which is a view of the scanner assembly looking aft. The 1.06 μm cw laser transmitter is shown in the center of the picture with the receiving detector at the top right center of the picture. The second laser transmitter (which is not part of the scanner assembly as shown) would mount on the shelf to the right of the picture in parallel with the other laser unit. Figure 14 is a view (looking aft in the aircraft) of the scanner assembly and its supporting electronics in three floor to ceiling racks. Two additional racks forward in the aircraft contain laser cooling equipment and the magnetic tape machine.

Figure 15 is a view looking forward in the aircraft showing one equipment operator taking a laser power output reading in the foreground while another makes a video gain adjustment at the operator electronic display and control panel. Note that both operators are wearing protective eye goggles and sound attenuating earphones. These protections are required when the lasers are operated because of the possibilities of stray laser radiation and the high noise level of the laser cooling equipment in the aircraft. The motion of the laser beam from either scanning or aircraft motion preclude an earthbound observer from eye damage from the laser during flight.

The scanner assembly is installed in the aircraft with a scan plane tilt 7^{o} aft of nadir to reduce specular surface reflection in the active band signals. The scan is at a constant angular rate from left to right across the aircraft ground track. The unobscured lateral scan field of view is 90^{o}.

The complete active/passive, multispectral scanner system weighs 2426 lbs and requires 16 KVA of electrical power. A breakdown of system weight by major assembly is presented in Table 10.

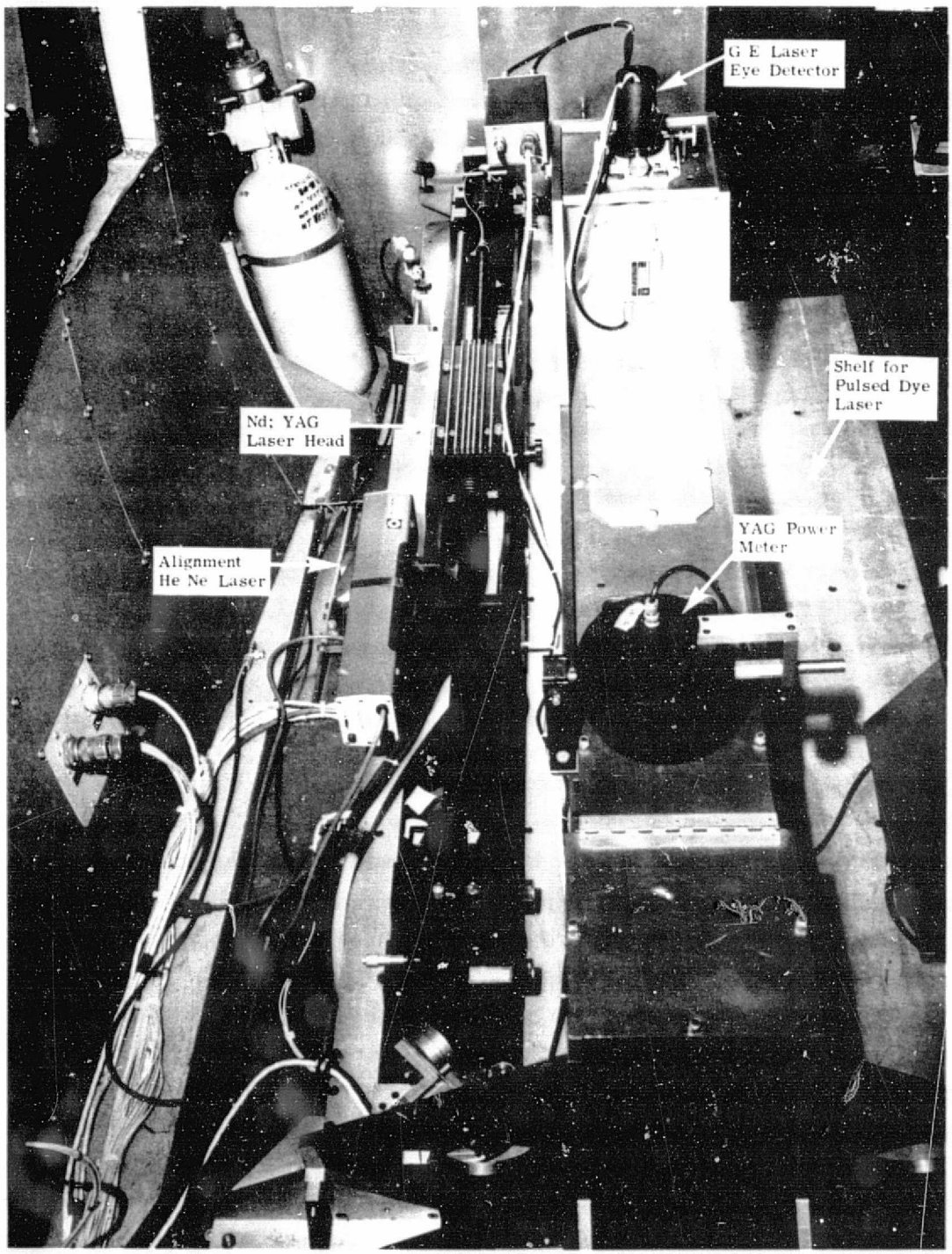

FIGURE 13. ACTIVE/PASSIVE MULTISPECTRAL SCANNER ASSEMBLY IN DC3C AIRCRAFT

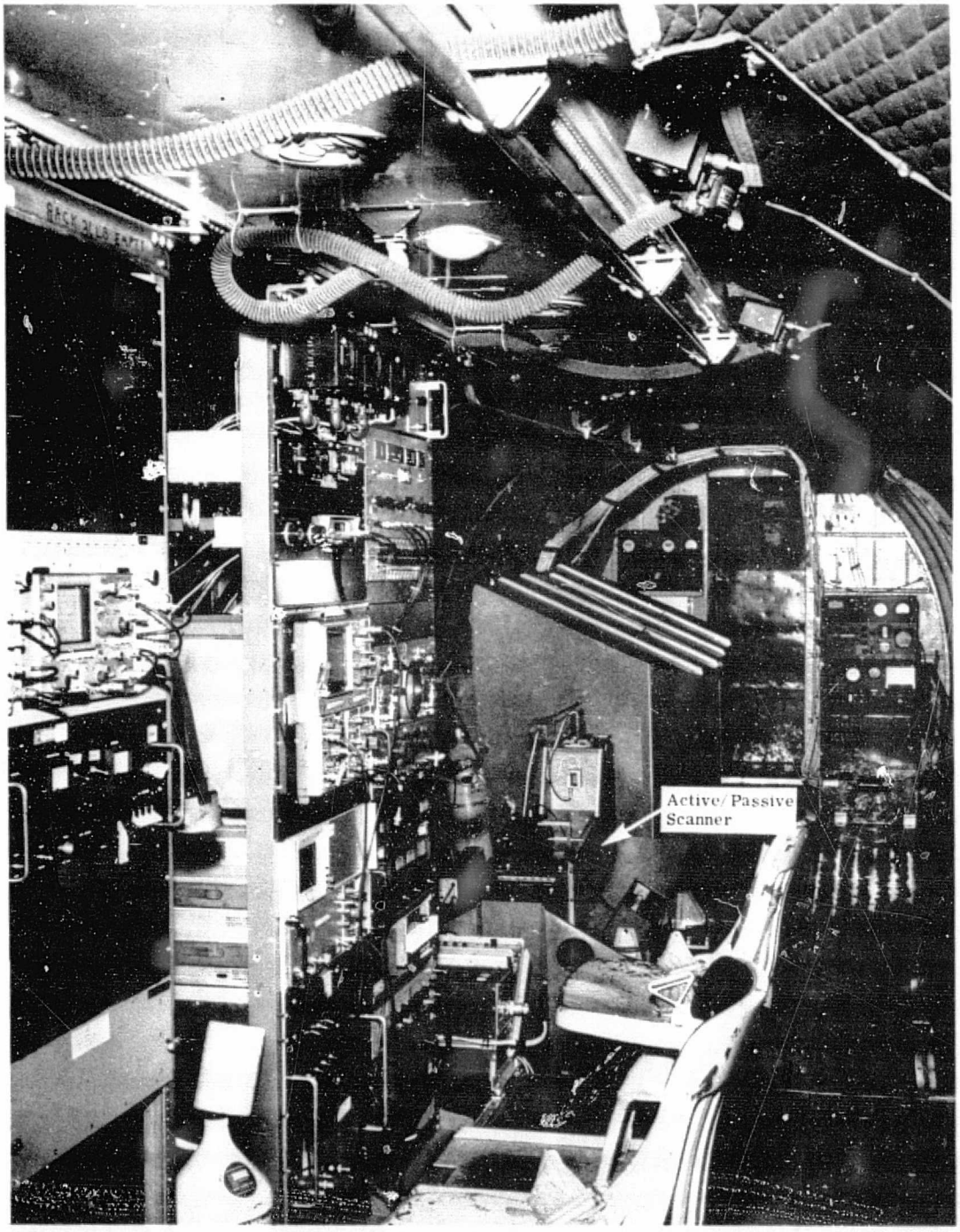

FIGURE 14. ACTIVE/PASSIVE MULTISPECTRAL SCANNER SYSTEM IN DC3C AIRCRAFT

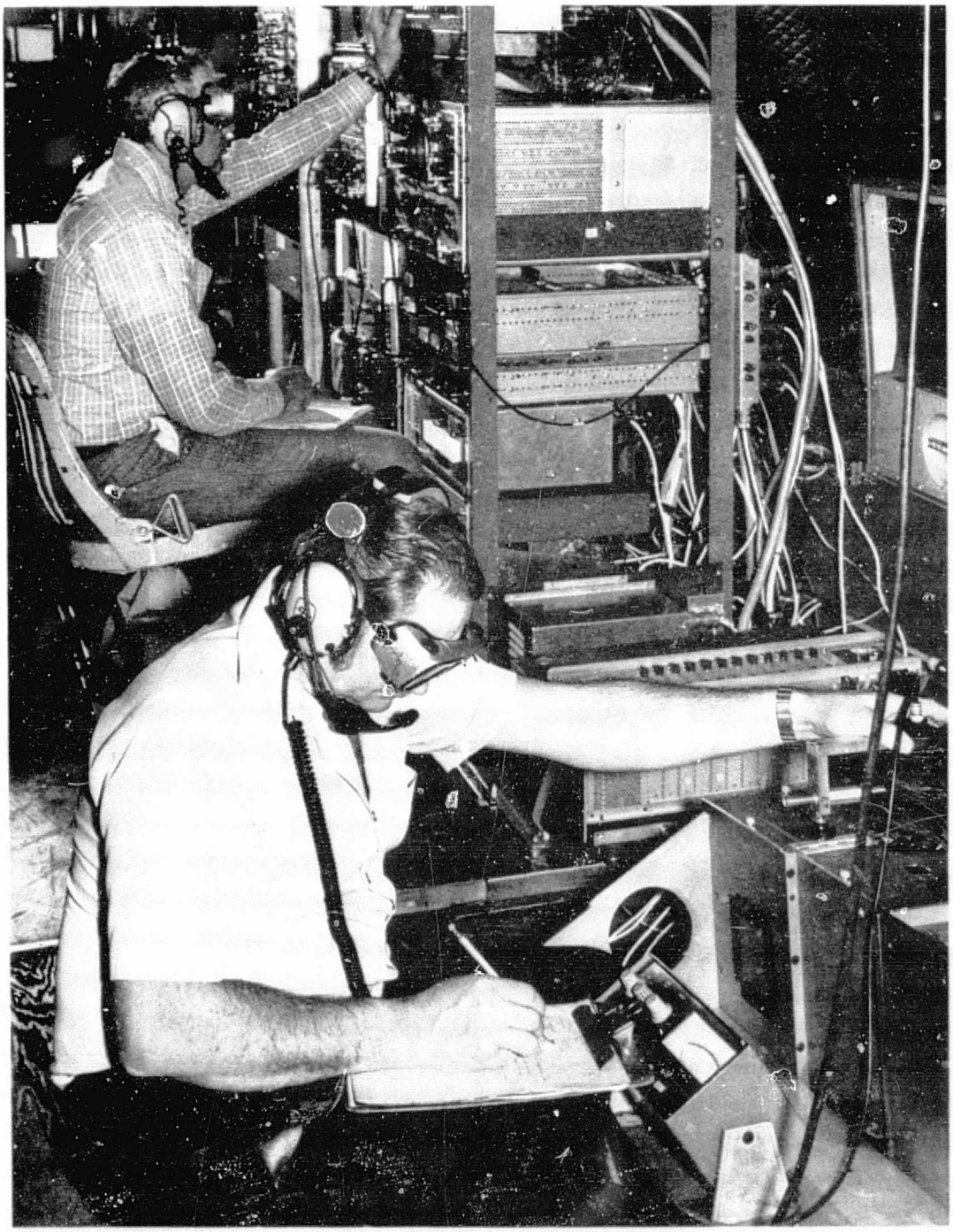

FIGURE 15. OPERATORS ADJUST ACTIVE/PASSIVE MULTISPECTRAL SCANNER IN AIRCRAFT

TABLE 10. ACTIVE/PASSIVE SCANNER SYSTEM WEIGHT

Rack 1	340 lbs
PC 500 Tape Machine	
Chiller	
Coolant	
Rack 2	380 lbs
Laser Cooler	
Distilled Water	
Heat Exchanges	
Rack 3	142 lbs
Laser Control Panel	
Oscilloscope (485)	
Power Supply	
Rack 4	285 lbs
Electronic Controls	
Camera Controls	
Monitor Oscilloscope (7904)	
Pulse Analyzer (605)	
Digitizer (R7912)	
Digital Record Unit	
Rack 5	236 lbs
Digital Voltmeter	
Digital Counter	
Video Postamplifiers	
Electronic Controls	
Monitor Oscilloscope (RM565)	
Scanner Control Unit	
Equalizers	
High Voltage Power Supply	
Low Voltage Power Supplies	
Scanner Assembly	781 lbs
Scanning Mirror Unit	
Collector Optics	
Spectrometer	
IR Detector	
Active Receivers	

TABLE 10. ACTIVE/PASSIVE SCANNER SYSTEM WEIGHT (Continued)

Scanner Assembly (Continued)	
Active Transmitters	
Video Preamplifiers	
Radiation Calibration Sources	
Miscellaneous	262 lbs
Scan Motor Control	
Power Amplifier for Black Bodies	
Cables	
Plumbing	
TOTAL	2426 lbs

3.

CONTRACT PERFORMANCE SUMMARY

This contract was initiated in June 1975 as an 18 month program with half a million dollar funding. The funding has remained the same but the contract completion has slipped four months because of delays in contract task accomplishment.

3.1 PROGRAM STATUS

The program originally consisted of six major tasks. The sixth task was dropped as a requirement when cost overruns occurred in the completion of the first five. The tasks are listed as follows:

1. System Analysis
2. System Design
3. Equipment Fabrication and Procurement
4. Equipment Assembly and Test
5. System Installation and Flight Test
6. Data Collection and Analysis.

At the close of the contract effort, an airborne system, configured as designed except for the absence of the pulse laser unit, was successfully test flown in ERIM's aircraft. The purchased pulse laser unit which had been physically integrated into the system was returned to the manufacturer prior to the flight test because of unacceptable performance during ground tests. This item was subsequently deleted as a deliverable part of the system.

The elimination of data collection and analysis as part of this contract effort has reduced the performance evaluation to a minimal effort. It is anticipated that other contracts will supply an acceptable pulse laser unit and will use the system capabilities to evaluate the potential of combined active and passive multispectral data in various applications.

3.2 DELIVERABLE ITEMS

Except for the performance evaluation reports associated with the deleted analysis task, all original contract items were delivered as planned. The delivered contract items are listed as follows:

1. Monthly Progress Reports
2. Monthly Financial Reports
3. Program Plan
4. Program Review at JSC
5. Design Study Report
6. Design Review at ERIM
7. Operating and Maintenance Instructions
8. Active/Passive Multispectral Scanner System
9. Final Report.

The Scanner System as delivered is a complete operational system except for the pulse laser unit, laser cooling provisions and data recording on magnetic tape. These capabilities are provided by ERIM in program sharing when the system is operated by ERIM in its aircraft.

APPENDIX A
COLLIMATOR BENCH TESTS

Throughout the assembly of the active/passive multispectral scanner, as each optical component was added to the system it was aligned with respect to numerous precision machined surfaces in the scanner frame. This was achieved using an autocollimation telescope and a HeNe laser. The overall alignment accuracy was on the order of a mrad or two. Once the components were in place and aligned as well as possible, the entire scanner was placed upon a collimator bench for alignment, resolution and registration tests. Since the active-transmit/passive-receive scan mirror and the active-receive scan mirror were separated by 24 inches at their centers, the collimator had to be used separately for each end of the scanner. Registration for the total system must therefore be left for the 1000 ft ramp tests.

The collimator bench consists of a Tungsten-Halogen lamp which illuminates a piece of diffuse reflecting flame-sprayed aluminum. Placed in front of the aluminum is a target consisting of an aperture or a series of three rectangular holes. These rectangular holes or bars allow measurement of the modulation transfer function or spatial resolution of the scanner receivers. In order to simulate the far-field, the aperture or 3-bar targets are placed near the focus of a 100 inch focal length paraboloid. Accordingly, each inch of target which can be resolved corresponds to a mrad of resolution for the scanner receiver.

As mentioned above, the scanner system was designed to provide 2 mrad resolution in all channels. The instantaneous field-of-view (IFOV) of each of the passive receivers is therefore 2 mrad and the laser transmitter beam is 2 mrad in angular extent. Although the total IFOV of the active receivers is greater than 2 mrad its effective IFOV or effective resolution is established by the laser beam size, i.e., 2 mrad.

Figure A-1 shows the results of the resolution tests performed on the collimator bench using 2 inch bars (holes) separated by 2 inch bars

(a) Photomultiplier Tube in Spectrometer

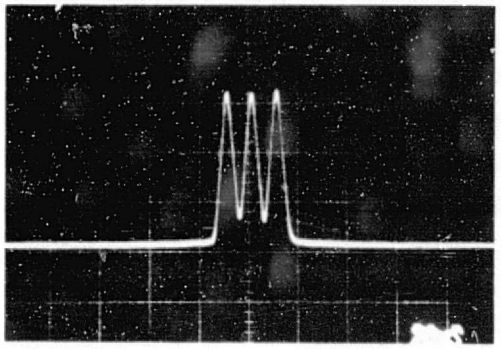

(b) HgCdTe Thermal Detector (9 - 11μm) in IR Channel

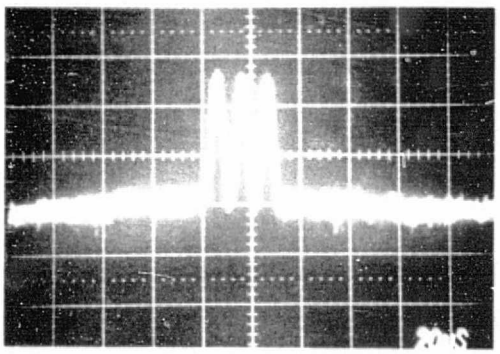

(c) Photomultiplier Tube, Pulse Receiver

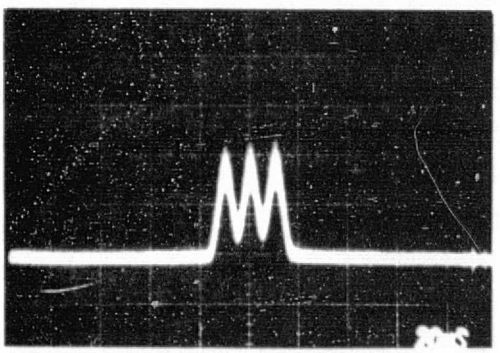

(d) Silicon Avalanche Photodiode, Active Imaging Receiver

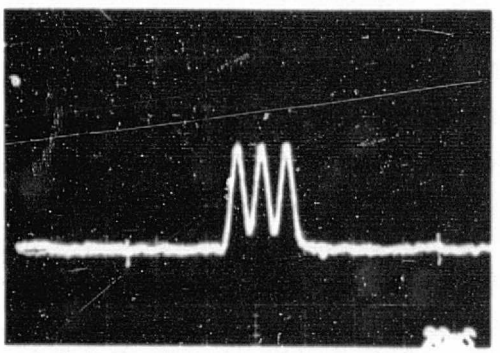

FIGURE A-1. RESOLUTION DETERMINATION USING A 2 mrad 3-BAR TARGET IN THE FAR-FIELD OF A 100 inch COLLIMATOR.

of flat-black painted aluminum to comprise a 2 mrad target. Resolution of (a) the spectrometer is nearly 2 mrad while that of (b) the thermal detector is clearly 2 mrad. The passive resolution of the active receivers can be seen in (c) and (d) to be greater than 2 mrad, but certainly less than the design of 3 mrad. This latter observation makes alignment of the active transmitters and receivers more critical but helps to reduce solar background slightly.

The bench collimator was also used to assure registration between the passive spectrometer, the IR receivers, and the active laser transmitter, all located on one end of the scanner. Figure A-2(a) and (b) show good registration between the IR receiver channel and the spectrometer receiver channels. In (a) a HgCdTe thermal detector (9-11 μm) is used in the IR channel and in (b) an InAs near-IR detector (1.4-1.8 μm) is used. In Figure A-2(c), the Quartz-Iodide lamp has been turned off, and the Nd:YAG laser transmitter is operating to illuminate the flame-sprayed aluminum behind the 3-bar target. The well resolved signal which appears in the figure indicates good overlap of the transmit and receive beams, both in time and in space.

(a) Registration Between IR Channel (HgCdTe) and Spectrometer (PM Tube)

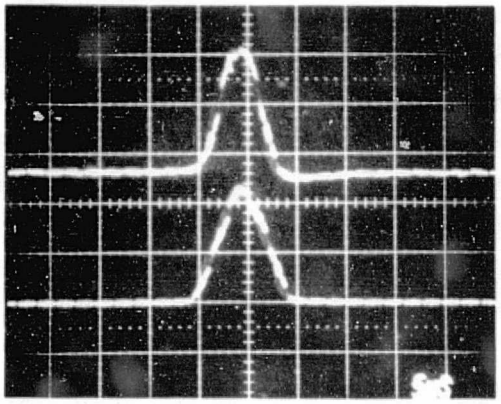

(b) Same Using InAs Detector in IR Channel

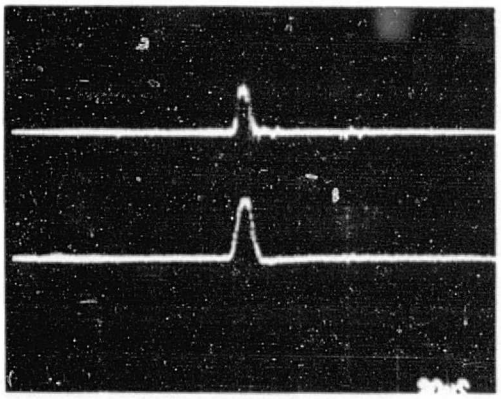

(c) Registration Between Nd:YAG Laser and IR Receiver (InAs, 1.0 - 1.4 μm)

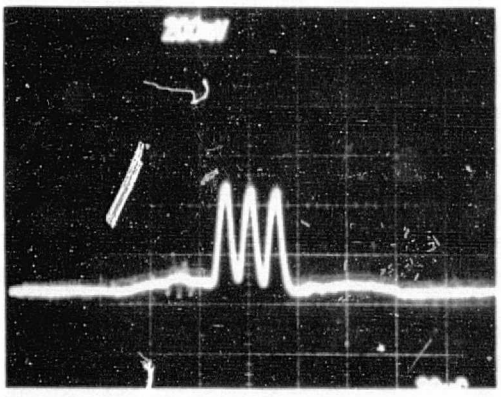

FIGURE A-2. REGISTRATION DETERMINATION USING THE 100 inch COLLIMATOR BENCH.

APPENDIX B

REFLECTANCE CALIBRATION OF ACTIVE SCANNERS

B.1 CALIBRATION SCHEMES FOR ACTIVE IMAGERY

Three internal calibration schemes for the active scanner bands were examined during the system development. The merits of the techniques considered for incorporation in the system are discussed herein.

Method 1: Monitor Laser Output Continuously

In this method a small fraction of the laser output is fed directly to a suitable calibration detector whose output is amplified and recorded in parallel with the receiver output of reflected radiation. During post-flight processing the calibration channel record is used to remove effects of variations in laser output. The great advantage of this scheme is that it monitors laser output throughout each scan. Its disadvantages are that it does not monitor receiver efficiency and, even as a monitor of transmitter output, it would be difficult and expensive to prevent drifts in gain of the calibration channel. Such drifts could occur due to changes in the beam dividing optics, detection responsivity, or electronic gain and would be interpreted as the reciprocal change in output of the laser. However such changes would occur quite slowly. Thus, this calibration scheme could provide a simple means of monitoring changes in laser output at high frequencies, particularly at frequencies higher than once per scan. As a result such a scheme would be complementary to one which can only follow changes at or below the scan rate.

Method 2: Monitor Transmitter to Receiver Path Once Per Scan

In this method an optical system accepts the laser beam reflected from its scan mirror during the inactive part of the scan cycle and

relays it to the receiver scan mirror. Typically the power reaching the receiver from a ground scene is on the order of 10^8 times less than that emitted by the receiver. In principle it would be possible to fix the attenuation of the relay optical path to this value to give an absolute end-to-end calibration. However, the difficulty of making an independent determination of the gain of the relay optics involved indicates that this is not practical. As a secondary calibration system, however, it would only be necessary to ensure relay gain stability at an appropriate level.

Method 3: Direct Monitor of Modulated Transmitter

It would be possible to modulate the small fraction of the laser output fed directly to the receiver so that the data signals and calibration signals could be separated during processing. However, the modulation frequency would have to be more than twice the signal data rate to avoid ambiguity. Elaborate and relatively expensive means such as an E-O modulation would be required and additional complexity would be introduced into the receiver recording and/or processing. No further consideration was given to this scheme because of its complexity.

B.1.1 Implementation of the Calibration Schemes

As an active scanner measures apparent* reflectance rather than apparent radiance it would, in principle, be possible to use an internal reflectance standard to provide an absolute calibration without the use of external primary standards. However, the dynamic range in power at the receiver is 10^{-10} to 10^{-8} of the transmitted power. Thus an absolute internal reflectance calibration scheme would require a known optical

* "apparent" in the sense that the actual reflectance is modified by absorption emission and scattering in the atmospheric path.

attenuation of this order of magnitude. Measuring the transmission of an optical system accurately is very difficult unless the system contains only flat surfaces and is free from scattering. On the other hand providing internal secondary calibration schemes to be standardized against external reflectance standards is very straightforward. Little attention has therefore been paid to absolute internal calibration schemes. Thus the two primary requirements for the schemes to be considered are that they cover appropriate dynamic ranges with adequate signal-to-noise and that they show high stability throughout the period between external calibrations.

Method 1. Continuous Monitor of Laser Output

Since very high powers are available at the transmitter a very simple calibration path optical system will suffice (except when modulation is required, see below). In fact calculations show that for a 20w Nd:YAG laser, a silicon diode could collect enough of the radiation scattered from one of the fixed folding mirrors to give more than adequate signal-to-noise without the use of special diverting optics.

However, if the laser is operating cw the radiation reaching the monitoring detector should be modulated to provide a zero reference level. This could be done at high frequency using an AO or EO modulator, but a fairly elaborate optical system would be required to obtain the narrow collimated beam such devices require. Alternatively a mechanical chopper could be used which blanked the beam once or twice per scan cycle (say 90° before and/or after nadir). This chopper would have to be synchronized with the scan, so again a relatively elaborate system is called for.

In any case a recorder channel would be required for each laser output monitor. However the data processing involved would be very simple.

Fortunately high frequency (>100 Hz) variations of the cw laser used in the system are sufficiently low that there is no need to introduce continuous monitoring of laser output.

Method 2: Periodic Monitor of Laser Output

The concept envisaged is illustrated in figure B-1. The path between transmitter and receiver is completed by the two 45° mirrors shown which face each other and which face the scan mirrors at some point during the scan dead time. The transmitter beam is expanded to fill the receiver aperture and, at the same time, is attenuated by two ground glass plates. The first plate is somewhat larger than the transmitter beam diameter d and second somewhat larger than the receiver diameter D. They are separated by a distance ℓ which can be varied by moving one of the plates. Suppose that the plates have diffuse transmittances τ_1 and τ_2 Str^{-1} respectively. [By diffuse transmittance we mean that if an irradiance E falls on one side, a radiance τE appears at the other. For an ideal diffusing screen with no losses $\tau = \frac{1}{2\pi}$. Real screens may have τ less or greater than this depending on whether more or less than half of the radiation is backscattered and also on the polar diagram of the scattering effect.]

Then if power ϕ_t falls on the first screen, the second screen sees an intensity $\tau_1\phi_t$ at the first screen giving an irradiance at the second screen of $\frac{\tau_1 \phi_t}{\ell^2}$. The radiance at the second side of the second screen is then $\tau_1 \tau_2 \phi_t/\ell^2$ and the power entering the receiver optics becomes

$$\phi = \tau_1 \tau_2 \phi_t \frac{\pi}{4} D^2\alpha^2/\ell^2$$

where α is the IFOV of the receiver.

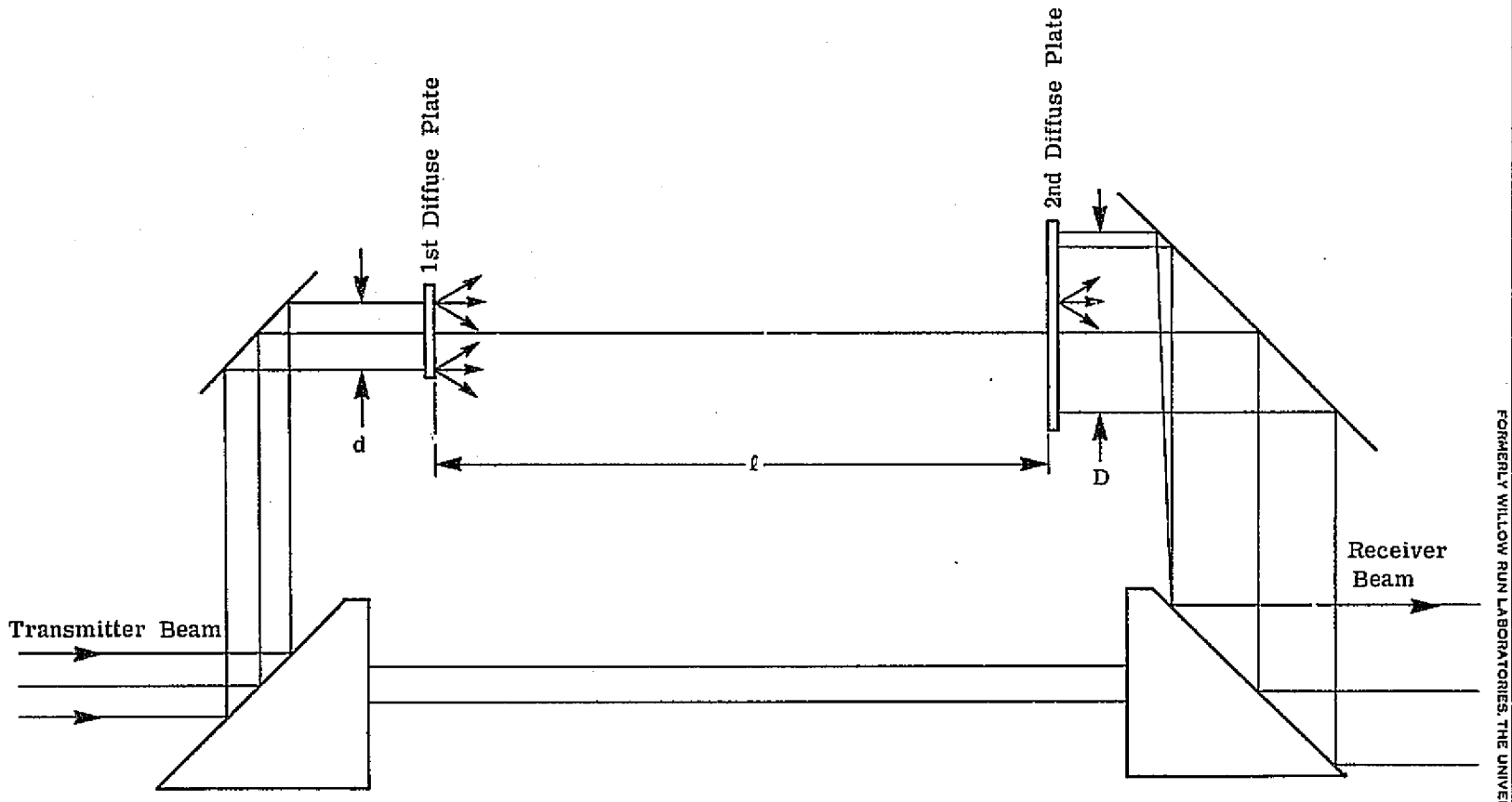

FIGURE B-1. CALIBRATION TRANSFER BEAM OPTICAL LAYOUT

Thus the gain of the calibration optics is

$$G = \phi/\phi_t = \frac{\pi}{4} \tau_1 \tau_2 \, D^2 \alpha^2 / \ell^2$$

Using expected values for the parameters as follows:

$\tau_1 = 1/2$

$\tau_2 = 1/2$

$D = 12.5$ cm

$\alpha = 0.002$ rad

$$G = 10^{-5}/\ell^2$$

Thus to obtain the gain of 10^{-8} indicated by the earlier discussion we must have

$$\frac{10^{-5}}{\ell^2} = 10^{-8}$$

$$\text{or } \ell = \sqrt{10^3}$$

$$= 32 \text{ cm} \quad (12.6 \text{ in.})$$

This is in fact a convenient distance as the separation of the two scan mirrors is to be about 18 in. The attenuation can be reduced by reducing ℓ, and increased by inserting neutral density filters or further ground glass plates. In fact the obvious procedure is to set $\ell = 18$ cm initially with adjustment to 10 to 32 cm allowing change in gain of $\sqrt{10}$ or $1/\sqrt{10}$ but setting the initial overall gain to the approximate magnitude required by experimenting with the fabrication procedures for the ground glass plates and possibly by introducing a neutral density filter if further attenuation is required.

This system would introduce a calibration signal into the receiver during the scan dead time to track slow variations in transmitter output and receiver sensitivity. Thus it will be a straightforward matter to use the calibration signals in post-flight processing to correct the data for changes in transmitter output and receiver sensitivity. However, calibration signals, having been reduced to the level of the scene signals, will be relatively noisy. But, the duration of the calibrate signals can be made equal to many resolution elements by ensuring that the first screen is somewhat larger than the diameter of the transmitter beam. Thus the effective signal to noise can be increased by smoothing either by gating the amplifier bandwidth to a smaller value during the calibrate period or by smoothing during processing.

An alternate concept of this technique is to use a fiber optic to direct a portion of the laser signal through attenuating filters into the receiver during the scan internal view.

B.1.2 Procedure for External Calibration

It is necessary to calibrate the active scanner for each altitude at which the scanner is to be operated and over the range of scan angles of interest. Figure B-2 illustrates a straightforward way in which this can be done on a horizontal or near horizontal test range. The range must be able to accommodate the maximum values of $h/\cos\alpha$ of interest.

In Figure B-2 the test target (of known reflectance properties) is shown angled to simulate the geometry of the airborne situation completely. This implies that a specific definition of reflectance and the bidirectional reflectance of the test targets be known for all angles of incidence of interest.

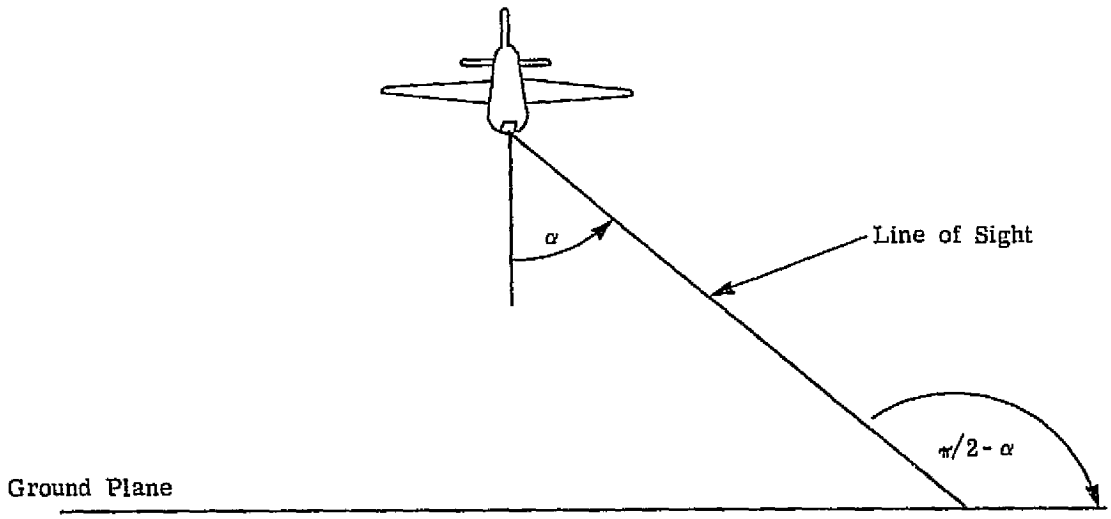

a. Flight Situation

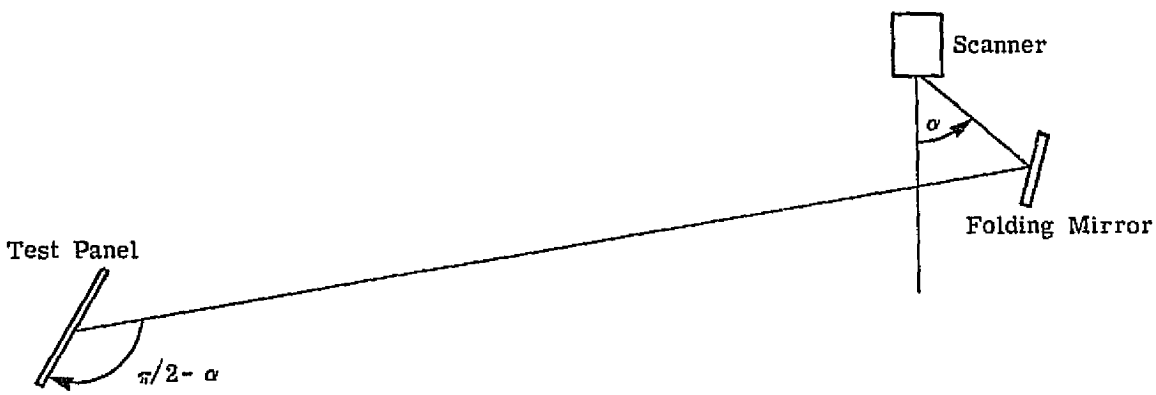

b. Test Range Situation

FIGURE B-2. GEOMETRY FOR EXTERNAL CALIBRATION

B.1.3 Calibration Accuracy Obtainable

A transfer optical system can track changes in efficiency of transmitter and receiver but not changes in internal geometry. Thus the sources of calibration error will be:

1. Uncertainty in reflectance of standard reflectance panels.
2. Electrical noise on calibration signal.
3. Instability of transmission of transfer optics.
4. Instability in scanner geometry.

Reflectance of Standard Target

The accuracy with which the bidircetional reflectances of the standard panels used is on the order of 3% of the indicated reflectance.

Noise on Calibration Signal

If the duration of the calibration signals is made about 5° of scan, the calibrate signal covers about 25 reselms. Thus when averaged over this angle the calibration signal should have a noise level $\sqrt{25}$ less than the data signals. Thus when added to the data signal noise during the calibration processing, the effect will be to increase the noise by 1/25. This is insignificant compared with other sources of uncertainty.

Stability of Transfer Optics

The geometric stability of the transfer optics depends on the separation of the diffusing plates. As this can easily be held to 1 part in 1000 (0.010" in 10") or better, no significant problem should arise here. However, degradation due to contamination of the optical surfaces could be a significant problem. It therefore is desirable to cover the entrance and exit ports of the transfer optics with glass plates which can be replaced or cleaned readily. The rest of the path should be sealed as far as this is practicable. In this way it should be possible to maintain adequate stability of this sub-system.

Stability of Scanner Geometry

The structure of the scanner is solid and that the various mirror mounts are rugged. Unfortunately, with the resources available it is impossible to do more than estimate the geometric changes which might occur under the vibration and thermal environments the system will experience.

The specifications for the scan mirror assembly require that the angle between the scan mirrors be stable to 0.1 mr at operating speeds.

If we assume that the structural stability of the rest of the system is comparable we arrive at an r.m.s. error in alignment between transmitted and received beams of 0.14 mrad. This is approximately 5% of the nominal IFOV of 3 mrad.

Overall Accuracy

As indicated in the preceding subsections, the two significant factors determining calibration accuracy are the accuracy with which the reflectivities of the external calibration panels are known and effects associated with the mechanical stability of the scanner. The effects are on the order of 3 and 5% respectively though the second figure is quite uncertain. The root of the sum of the squares of the two figures is about 6% which is thus the best estimate we can give for the overall uncertainty of the calibration scheme. However, it is recommended that the system be recalibrated on the test range as frequently as practicable. In this way, a good indication of the mechanical stability of the instrument will be obtained and the effects of any instabilities present on calibration accuracy determined.

B.2 CALIBRATION OF THE DEPTH SENSOR

The depth sensor is a pulsed, tunable laser radar system, operable at 0.53 nm and 0.64 nm. The return from it is examined for pulse dispersion (i.e., pulse spreading) as a means of determining both the range of depths from which returns are received, and the effective bulk scattering coefficients of the medium from which returns are obtained. Accurate altitude information is needed to obtain absolute reflectance from either this sensor or the active imaging sensor; the time delay between the transmitted pulse and the first return from the bulk scattering will give accurate information concerning air-craft altitude. It is the purpose of this section to describe the calibration needed for this sensor in order to maximize the accuracy of the information obtained on depth, altitude, and bulk reflectance properties.

B.2.1 Expected Returns

We currently envision the return obtained from this system, as seen in the photomultiplier tube current, to consist of an irregularly shaped pulse made up of the sum of the returns from the various layers in the partially transparent medium under study. Figure B-3 shows an example of such a return. The returned signal is the integral of the contributions from each layer. Each contribution appears at the detector at the time after pulse transmittal corresponding to the round trip time for that layer.

An examination of the integral involved shows that individual portions of the return can be unambiguously assigned to layers only if the pulse duration is shorter than twice the time required for a pulse to traverse one layer. Therefore, if we desire a depth resolution of one foot in water we need a pulse shorter than twice the time it takes light to travel one foot in water. We need a pulse shorter than 2.7 nsec.

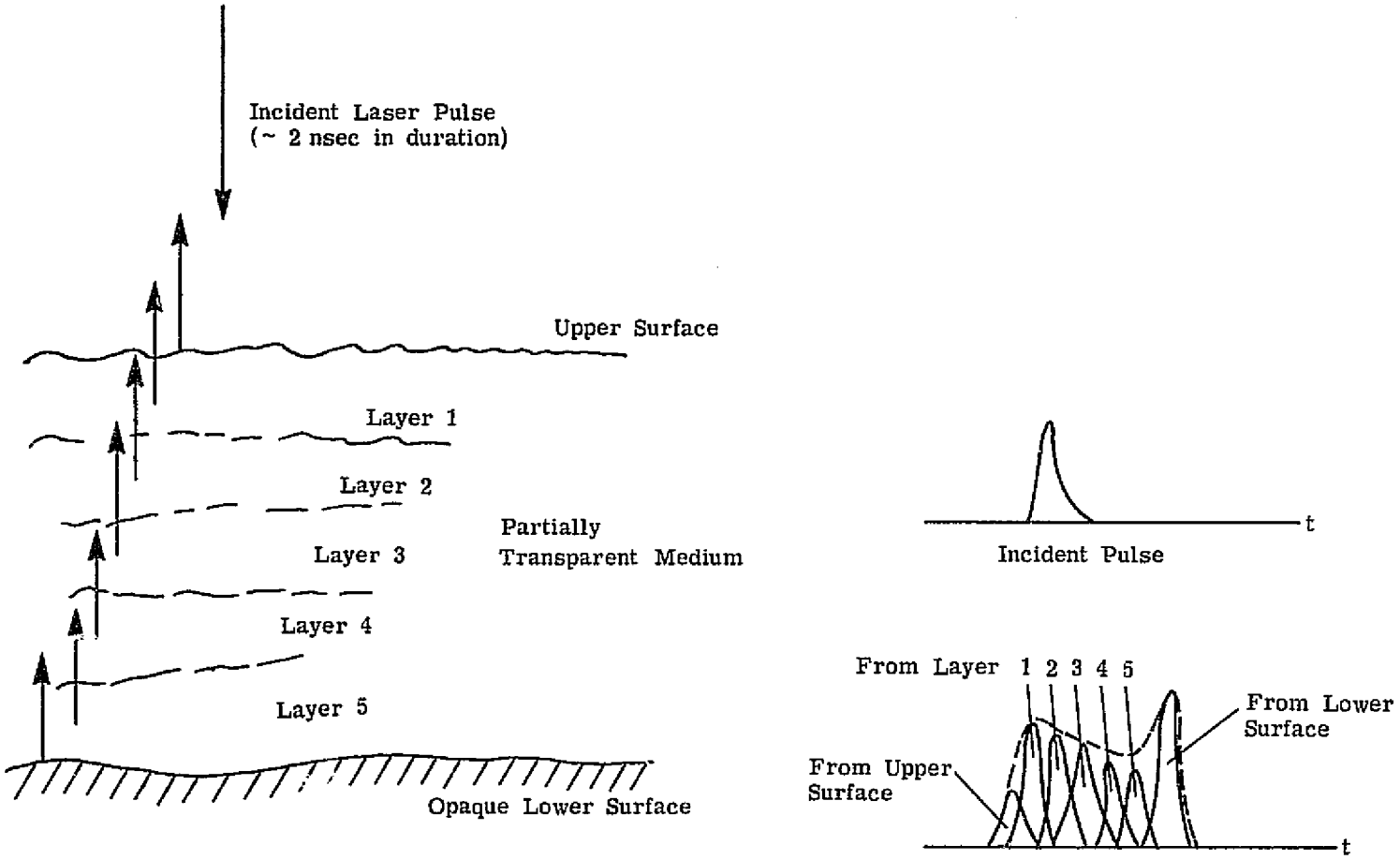

a. Partially Transparent Medium Illuminated By Laser Pulse

b. Temporal Shape of Incident and Return Pulse

FIGURE B-3. EXPECTED RETURN FROM DEPTH SENSOR

B.2.2 Expected System Design

The pulsed laser is expected to have a pulse width of approximately 6 nsec and a peak power of about 15 Kw. Thus we expect to attain range resolution of about two feet in water.

We expect that the output energy of this laser will vary by about 3% from pulse to pulse, and individual measurements of pulse energy will be needed to maximize the accuracy of bulk reflectance measurements. It is assumed that the effective duration of every pulse will be the same. This will simplify the monitoring of laser output required. During testing the uniformity of pulse duration will be measured to determine the validity of this assumption.

We expect that this laser will operate in the TEM_{00} mode so that the output pattern, or beam profile, from the laser will be uniform from pulse to pulse. It is also expected that the polarization state of this system will be uniform, so that polarization effects in this sensor will be minimal.

In order to perform the tasks required of the sensor, the system will be designed substantially as shown in Figure B-4. The nadir-sensor will trigger the laser and open a gate to enable both a laser pulse energy measurement circuit and a counter to record the time between transmitted and received pulse (for altitude measurement). A fiber optic coupling will be used to couple a very small fraction ($\sim 10^{-7}$) of the laser output to the primary PMT detector. One of the attenuating members in this beam will be adjustable to allow a suitable sampling level to be obtained at the detector.

The extent and frequency with which the attenuator in the laser sampling beam will need adjustment can only be determined by experience. If the amplitude of the returns from the various scenes under study is substantially variable, it will probably be necessary, in order to obtain proper triggering of the counter, to vary the gain of the PMT system and

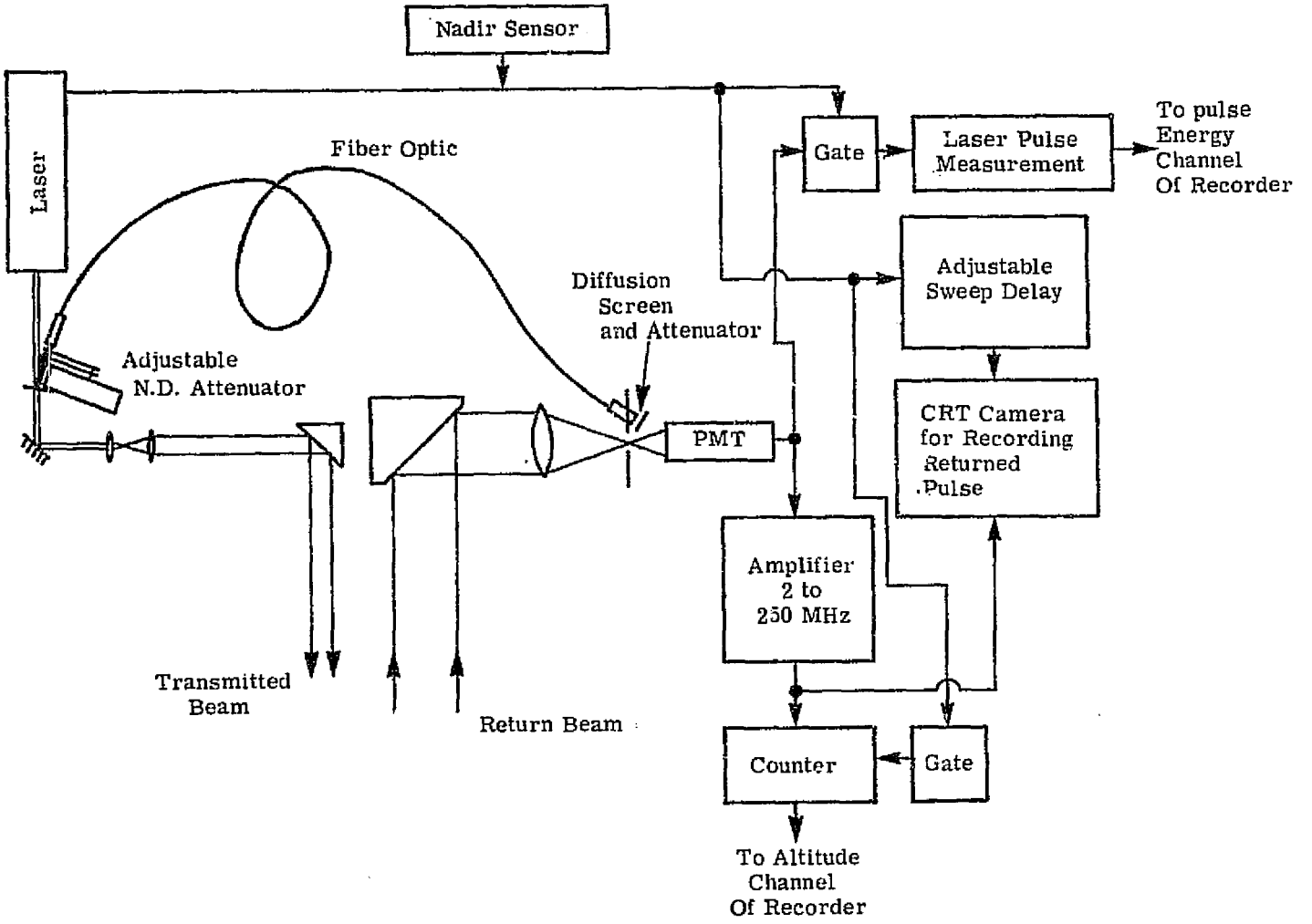

FIGURE B-4. BLOCK DIAGRAM OF DEPTH SENSOR

the amplitude of the transmitted beam as sampled by the PMT. This will require at least a relative calibration of this attenuator if the PMT is to be used as a primary power meter. On the other hand, if the amplitude of the return is constant or if the PMT electronics can be made to trigger reliably over a large dynamic range, then the attenuator will not need frequent adjustment.

B.2.3 Radiometric Calibration Required

The voltage output of this sensor can be described as:

$$V(t) = \frac{g^2}{h^2}\,\phi\,\rho'\,f_1(h,\ \text{alignment},\ t) \qquad (1)$$

where g = path absorption
h = path length (altitude)
ϕ = transmitter power
ρ' = scene reflectance

Here f_1 is a responsivity. Since this device will look only at nadir, the scan angle dependency does not appear. But the overall responsivity of the system does depend on the alignment achieved between transmitter and receiver optics and how this alignment, and the resulting integral of the beam profile of the laser and the sensitivity contour of the receiver, change with altitude. A long-term dependence in this function is also included to account for long-term calibration drift. In Equation (1), the assumption that variations in laser power do not affect the beam profile allows a factor ϕ to be taken out of the integral.

ρ' in Equation (1) signifies the effective bidirectional reflectance from the bulk medium in this case. For the case where the pulse duration of the laser is much less than the depth resolution required (translated to twice the travel time) the effective ρ' can be written

$$\rho_{eff}(t) = \frac{\int\phi dt}{\phi}\,\frac{\tau^2(t)k_s(t)}{n(t)}\,\frac{C}{2} \qquad (2)$$

where k_s is the bulk bidirectional reflectance of the medium in units of $sr^{-1}cm^{-1}$, n is the index of refraction of the medium and τ is the transmittance from the upper surface of the medium. The time dependence signifies that the apparent bidirectional reflectance is a function of time in the return and determines the value of the product $\tau k_s/n$ at that time (or distance into the medium). The velocity of light is c. Note that the integral of the power in the pulse is now required rather than the instantaneous power. Substitution of this quantity into Equation (1) yields

$$V(t) = \frac{g^2}{h^2}\left(\int \phi dt\right) \frac{\tau^2(t)k_s(t)}{n(t)} \frac{c}{2} f_1 \text{ (h, alignment, t)} \qquad (3)$$

Note that the time dependence in f_1 is on a much longer time scale than the duration of the return so that variations in f_1 need not be accounted for in any given return.

For every pulse, a return will also be obtained from the laser pulse measurement channel. A single output value, V_L, is to be obtained proportional to the integrated laser power.

$$V_L = f_2(t)A_N A_F(t) \int \phi dt \qquad (4)$$

Here f_2 is the responsibity integral for this channel, which is assumed susceptible only to long-term drift (alignment of the fiber optic coupling system is to be well fixed). A_F is the attenuation of the fiber optic coupling system, also susceptible to long term drift due to contamination. A_N is the attenuation of the adjustable neutral density filter. Time drift in this quantity can be lumped into that of A_F.

Values for the product $\tau k/n$ can be obtained from the output by substituting the integral $\int \phi dt$ from Equation (4) into Equation (3) as follows:

$$\frac{\tau(t)k(t)}{n(t)} = \frac{V(t)}{V_L}\frac{h^2}{g^2}\frac{2}{c}\frac{A_N A_F(t) f_2(t)}{f_1(h,\ \text{alignment},\ t)} \tag{5}$$

The quantities h^2 and g^2, and c are expected to be determined by other means, so that it is the purpose of calibration to determine the quantity

$$\frac{A_N A_F(t) f_2(t)}{f_1(h,\ \text{alignment},\ t)}$$

This quantity can be determined for any one time, attenuator setting altitude, and alignment by calibration using the same ground range described in the preceding section (see Figure B-2). This calibration can be performed with the scanner stationary and the laser triggered from a 100 Hz signal generator.

During such a calibration, the return will consist of a reflection from the calibration panel of known bidirectional reflectance, ρ_c', at known distance h_c. ρ_c' will be chosen to reproduce the signal levels to be expected from the typical water returns. Presumably the atmospheric transmittance, g_c can be determined with sufficient accuracy also. The voltage output will be

$$V_c(t) = \frac{g_c^2}{h_c^2}\phi(t)\rho_c' f_1(h,\ \text{alignment},\ t) \tag{6}$$

The corresponding output from the laser pulse measurement channel will again be given by Equation (4), so that the required calibration quantity

$$\frac{A_N A_F(t) f_2(t)}{f_1(h,\ \text{alignment},\ t)} = \frac{V_L}{V_c(t)dt}\rho_c'\frac{g_c^2}{h_c^2}$$

Note that the calibration requires an integral of the voltage output from the calibration return. Although the temporal response of the electronics associated with the return will not be sufficient to resolve the pulse width, we assume that the electronics comprise a linear system so that time integrals are preserved.

At the time of calibration, data can be collected at various settings of the attenuator, A_N; calibration is thus preserved as A_N is varied.

If it is possible to assume that drifts in the responsivity of the receiver with time do not affect either the sensitivity contours of the photomultiplier, or the characteristics of receiver components other than the photomultiplier, then much of the time variation in the combined calibration quantity will vanish ("cancel out") of the calibration quantity. Drifts of this type in the PMT and its associated electronics will indeed be the primary cause of long-term drift. Thus the need for recalibration will be determined more by possible contamination of the optics rather than by variations in PMT response with time. As with the other active channel, protection of the optics from contamination by dirt and dust is important in maintaining the calibration of the system. It is estimated that relative radiometric errors will keep the accuracy of the over-all reflectance calibration to the order of 10% (excluding altitude effects).

B.2.4 Time Calibration Required

In order to reduce any of the received signals to reflectance values, an accurate altitude for the aircraft is required. This can be obtained from the time delay between transmitted and received pulse. The counting circuit shown in Figure B-4 is reset and enabled by a pulse from the laser triggering circuit, started by the leading edge of the pulse from the laser sampler and stopped by the leading edge of the return pulse. Signal-to-noise ratios will need to be as high as possible to allow unambiguous triggering of this clock by the returns.

Adequate time accuracy for this counter can be easily obtained by the use of a crystal controlled clock. However, because of the short pulse durations and time accuracies required, as high a clock rate as possible will be required. If we use a clock frequency as high as 125 MHz, we will obtain altitude accuracy no better than one clock bit, or

eight feet. This is adequate for reduction of the radiometric data to reflectance since it represents an error in range-squared of 1.6%, which is significantly better than one can expect for the radiometric errors. Compared to 1.6%, the error in the clock frequency itself is expected to be negligible.

The other time variable of importance is the time axis of the return display. Commercially available hardware is used for this task with specifications adequate to allow relative time identification of the contents of the return. This requires accuracy sufficient to measure 1 nsec in the duration of the return (say 30 nsec). This places an accuracy requirement of only 3% on the rate of sweep. But in order for sequential returns to appear at predictable, non-varying positions on the screen, the delay between the pulse transmittal and the start of the display sweep must be uniform from pulse to pulse within 1 nsec. We need to obtain delays of the order of 2 μsec which are accurate and uniform to within 1 nsec. This may prove to be a difficult requirement to meet.

B.2.5 Conclusions Regarding Calibration of the Depth Sensor

We have described a calibration technique for the depth measuring sensor which will allow the examination of the dispersion in the return from a pulsed optical radar to be used to infer scattering coefficient as a function of depth to an accuracy of about two feet. In addition the device is capable of measuring the range to the upper surface generating the return to within an accuracy of about eight feet.

REFERENCES

1. P. G. Hasell, Jr., et al., Michigan Experimental Multispectral Mapping System, A Description of the M7 Airborne Sensor and Its Performance, Report No. 190900-10-T, Environmental Research Institute of Michigan, Ann Arbor, Michigan, January 1974.

2. F. J. Thomson and P. G. Hasell, Jr., et al., Design Study Report: Active and Passive Multispectral Scanner for Earth Resources Applications (An Advanced Applications Flight Experiment), Volumes I - Application Analysis, II - Calibration Analysis and III - System Concept, Report No. 115800-8-T, Environmental Research Institute of Michigan, Ann Arbor, Michigan, November 1975.